



**HAL**  
open science

## Rapid earthquake response: The state-of-the art and recommendations with a focus on European systems

Simon Guérin-Marthe, Pierre Gehl, Caterina Negulescu, Samuel Auclair,  
Rosemary Fayjaloun

### ► To cite this version:

Simon Guérin-Marthe, Pierre Gehl, Caterina Negulescu, Samuel Auclair, Rosemary Fayjaloun. Rapid earthquake response: The state-of-the art and recommendations with a focus on European systems. International Journal of Disaster Risk Reduction, 2020, 52, pp.101958. 10.1016/j.ijdr.2020.101958 . hal-03742057

**HAL Id: hal-03742057**

**<https://brgm.hal.science/hal-03742057>**

Submitted on 2 Aug 2022

**HAL** is a multi-disciplinary open access archive for the deposit and dissemination of scientific research documents, whether they are published or not. The documents may come from teaching and research institutions in France or abroad, or from public or private research centers.

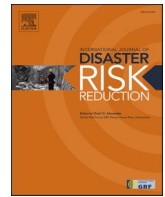
L'archive ouverte pluridisciplinaire **HAL**, est destinée au dépôt et à la diffusion de documents scientifiques de niveau recherche, publiés ou non, émanant des établissements d'enseignement et de recherche français ou étrangers, des laboratoires publics ou privés.



ELSEVIER

Contents lists available at ScienceDirect

## International Journal of Disaster Risk Reduction

journal homepage: <http://www.elsevier.com/locate/ijdr>

Review Article

## Rapid earthquake response: The state-of-the art and recommendations with a focus on European systems

Simon Guérin-Marthe<sup>\*</sup>, Pierre Gehl, Caterina Negulescu, Samuel Auclair, Rosemary Fayjaloun

BRGM, Orléans Cedex, France

## ARTICLE INFO

## Keywords:

Earthquake rapid response  
Shake-map  
Damage estimation  
Loss assessment

## ABSTRACT

Systems for Rapid Response to Earthquakes (RRE) aim at providing reliable and near-real time ground-motion and loss estimates following an earthquake, in order to help authorities taking appropriate actions when needed. The purpose of this study is to review the state-of-the-art for RRE systems, focusing first on the tools and methods that have been developed for shake-map computation (i.e., taking into account the seismic recordings as well as macroseismic observations when available), in order to provide a map of the ground shaking intensity rapidly after an earthquake event. The second part focuses on the different approaches taken for rapid loss assessment, the ones based on shake-maps and the others. We give an overview of the current operating systems with emphasis on European ones, and we highlight their differences and identify the current gaps and pending issues. Finally, we call attention for the need to treat carefully uncertainties propagated at each calculation step, which added up are non-negligible, and are an important part of the result itself. Considering the full statistical distribution of loss and damage estimates provides more information than average or median values, and such statistics should therefore be provided by RRE systems and taken into account by decision-makers in order to take informed actions following an earthquake.

## 1. Introduction

While earthquakes remain unpredictable, their impact on populations can be significantly reduced by taking appropriate and timely actions following strong ground motions. Updated damage and loss assessment can be performed in near-real time by using recordings from seismic stations, by using felt intensity observations such as “Did You Feel It” (DYFI) reports [1,2], or even by using large amount of data from social media such as Twitter in order to refine areas of felt intensity [3]. The updated spatial field of ground-motion parameters may in turn be used as an input to damage and loss assessment software, provided that exposure or vulnerability models are available for the affected area. This chain of tools and calculations, from acquiring seismic data to assessing the damages and losses, constitutes the backbone of Rapid Response to Earthquake (RRE) systems. The most pressing need is to optimize the resources available, allocating them strategically on the affected territories for an optimal response to the earthquake. Emergency systems must also be triggered in order to avoid secondary risks linked to transportations, or gas and oil lines, prioritizing inspection, shutting them off when needed, and letting them run when possible, in order to

facilitate rescue operations.

This paper, discussing the state-of-the-art approaches and recent developments in RRE systems, is written as a “traditional literature review” [4]. It is composed of two parts: the shake-map systems (Section 2), and the loss assessment systems (Section 3). The shake-map systems are discussed in term of the different algorithms used, as well as their respective input data. We present the equations of several algorithms used to compute shake-maps: the U.S. Geological Survey (USGS) ShakeMap® version 3.5 [5] and version 4 [6], and a Bayesian inference method [7]. We use Erdik et al. [8] as a basis for the inventory of loss assessment systems, and we detail the methods used for damage estimates. Although we give more emphasis on systems operating in Europe, we also briefly review more global ones which often constitute a basis and reference for other RRE systems. Finally, we discuss the possible improvements and pending issues of the current systems, in particular, how treating uncertainties and collecting a large amount of data can improve rapid loss assessment.

<sup>\*</sup> Corresponding author.

E-mail address: [simon-gm@hotmail.fr](mailto:simon-gm@hotmail.fr) (S. Guérin-Marthe).

## 2. Rapid ground shaking intensity assessment

This section details the current shake-map methods that are available, first summing up the underlying algorithms (Section 2.1), and then providing a comparative analysis of the systems in place (Section 2.2).

### 2.1. Shake-map algorithms

When an earthquake is detected, the magnitude and the location of the hypocenter are estimated. A Ground Motion Model (GMM), also called Ground Motion Prediction Equation (GMPE), is then applied in order to estimate ground-motion parameters around the hypocenter (each GMM having specific validity criteria such as magnitude range, fault mechanism and dimension, distance to the source, geodynamical context). The observations recorded during the event (i.e., ground-motion measurements and macroseismic intensities when available) are collected, sometimes corrected from the site amplification factors (in order to revert the measurements from soil conditions to rock conditions), and used to update the distribution of the ground-motion field (see Fig. 1). The latter result is called a shake-map, which is an estimate of the ground motion usually in the form of intensity measures (IMs) such as PGA (Peak Ground Acceleration), SA (Spectral Acceleration), PGV (Peak Ground Velocity) or macroseismic intensity. In the case macroseismic intensities are exploited as observations, a Ground-Motion-Intensity Conversion Equation (GMICE) is used in order to obtain ground-motion estimates. At the end, if the observations have initially been corrected for site amplification, the amplification factors are applied at each grid point (Fig. 1), in order to revert the ground-motion parameters from rock conditions to the actual soil conditions of the area.

The following section presents the main algorithms used to generate shake-maps, taking observations and uncertainties into account: the USGS ShakeMap® algorithms [5,6] and the Bayesian inference method [7].

#### 2.1.1. USGS ShakeMap® algorithm

The most widespread and elaborate shake-map system is the one operated by the USGS, thanks to developments by Wald et al. [5,9].

The still widely used version 3.5 is based on a weighted interpolation algorithm [10]. At the locations of observations, the global bias introduced by the observations with respect to the initial GMM estimates is computed: the bias is corrected by finding the magnitude that reduces the errors between the observed and the predicted ground motions,

when the GMM is evaluated for the adjusted magnitude. The bias-adjusted GMM is applied in order to estimate corrected ground parameters over a spatial grid. At each grid point, the ground-motion parameter of interest is updated through a weighted average between the bias-adjusted GMM estimate and the interpolated observations: the GMM estimate is weighted by the inverse of the variance provided by the GMM, while each observation is weighted by the term  $1/\sigma_{obs}^2$  (i.e.,  $\sigma_{obs}$  is the standard deviation assigned to the observation - it increases with the distance between the observation and the grid point, based on a ground-motion spatial correlation model).

Based on the interpolation scheme proposed by Worden et al. [10]; the mean updated ground-motion parameter  $Y$  at grid point  $(x,y)$  is expressed as:

$$Y_{xy} = \frac{\frac{Y_{GMM,xy}}{\sigma_{GMM}^2} + \sum_{i=1}^n \frac{Y_{obs,xy,i}}{\sigma_{obs,xy,i}^2} + \sum_{j=1}^m \frac{Y_{convobs,xy,j}}{\sigma_{convobs,xy,j}^2}}{\frac{1}{\sigma_{GMM}^2} + \sum_{i=1}^n \frac{1}{\sigma_{obs,xy,i}^2} + \sum_{j=1}^m \frac{1}{\sigma_{convobs,xy,j}^2}} \quad (1)$$

where  $Y_{GMM,xy}$  is the bias-corrected GMM estimate at the point  $(x,y)$  and  $Y_{obs,xy,i}$  (resp.  $Y_{convobs,xy,j}$ ) is the  $i$ th ground-motion measurement out of  $n$  (resp. the  $j$ th macroseismic observation out of  $m$ ) scaled to the point  $(x,y)$ . The scaling from the observation's location to each grid point  $(x,y)$  is performed using the relative source-to-distance factors provided by the GMM:

$$\begin{cases} Y_{obs,xy,i} = Y_{obs,i} \times \left( \frac{Y_{GMM,xy}}{Y_{GMM,obs,i}} \right) \\ Y_{convobs,xy,j} = Y_{convobs,j} \times \left( \frac{Y_{GMM,xy}}{Y_{GMM,convobs,j}} \right) \end{cases} \quad (2)$$

Similarly, the total variance of the updated ground-motion parameter  $Y$  at grid point  $(x,y)$  is expressed as:

$$\sigma_{Y,xy}^2 = \frac{1}{\frac{1}{\sigma_{GMM}^2} + \sum_{i=1}^n \frac{1}{\sigma_{obs,xy,i}^2} + \sum_{j=1}^m \frac{1}{\sigma_{convobs,xy,j}^2}} \quad (3)$$

where  $\sigma_{GMM}$  is the standard deviation of the intra-event error term associated with the GMM: when enough observations are present, it is assumed that the inter-event error term is well enough constrained by the bias correction.  $\sigma_{obs,xy,i}$  is the standard deviation associated with an observation location at a given distance  $d$  from the grid point  $(x,y)$ : for instance,  $\sigma_{obs,xy,i} = \sigma_{GMM} \cdot f(d)$ , where  $f$  is decreasing function with distance  $d$ . Usually, if  $d$  tends towards zero,  $\sigma_{obs,xy,i}$  tends towards zero (i.e., the observed value becomes the dominant term in near field); and if  $d$  tends towards infinity,  $\sigma_{obs,xy,i}$  tends towards infinity (i.e., the GMM

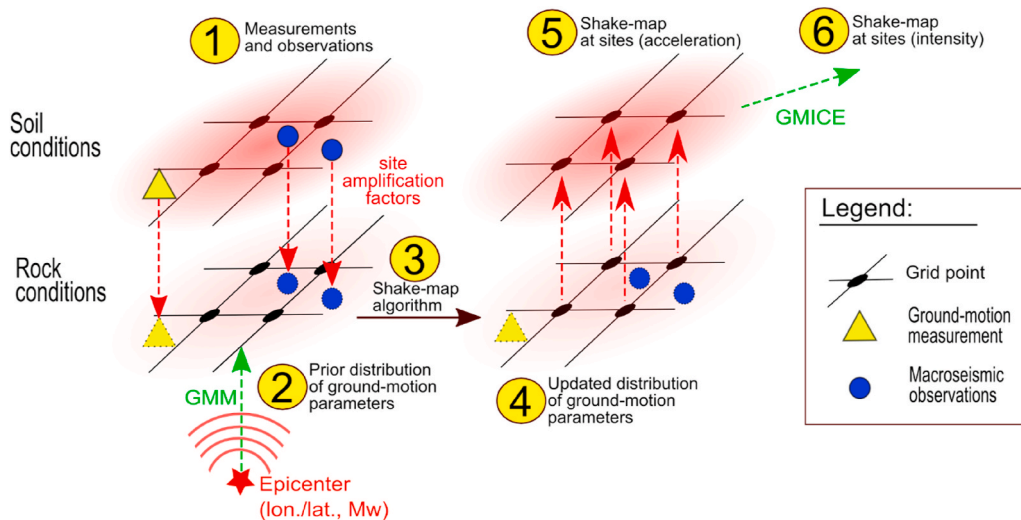


Fig. 1. Schematic main principles of ShakeMap® v3.5 and the Bayesian inference shake-map procedures. ShakeMap® v4 does not correct to rock conditions before interpolation.

estimate becomes the dominant in far field). The functional form and values taken by  $f$  depend on the spatial correlation model that is associated with the ground-motion parameter of interest. By default, Worden et al. [10] propose a radius of 10 km, within which we have  $\sigma_{obs,xy,i} < \sigma_{GMM}$ ; another radius of 15 km is defined, beyond which it is assumed that  $\sigma_{obs,xy,i} = \infty$ . The radius of influence of observations has a strong influence on the local shape of the shake-map; and further sensitivity studies should be performed in order to assess its link with the spatial correlation of the ground-motion parameters.

On the other hand, the standard deviation  $\sigma_{convobs,xy,j}$ , related to the uncertainty associated with macroseismic observations, is decomposed into the distance-based standard deviation  $\sigma_{obs,xy,j}$  (as detailed above), and the standard deviation of the Ground Motion to Intensity Conversion Equation (GMICE) (i.e. uncertainty from converting the macroseismic intensity into a ground-motion parameter):

$$\sigma_{convobs,xy,j}^2 = \sigma_{obs,xy,j}^2 + \sigma_{conv}^2 \quad (4)$$

The simple equations used by the algorithm prevent the build-up of computational complexity, since the optimization of Eq. (1) allows the computation time to remain linearly proportional to the number of grid points [10]. This shake-map system is flexible enough to produce updated maps of various types of ground-motion parameters (e.g., PGA, PGV, SA at different periods), as long as the ad-hoc GMMs are available. Shake-maps in terms of macroseismic intensity are also provided, thus making a direct use of the macroseismic testimonies that are collected after the earthquake event.

It should be noted that the recent version change of ShakeMap® (from version 3.5 to 4) has introduced a different interpolation scheme ([5]; [99]), namely the use of the multi-variate normal (MVN) distribution [11,12]. The vector of ground-motion parameters  $\mathbf{Y}$  (assumed to be normally distributed) is divided into  $\mathbf{Y}_1$  ( $m$  prediction sites, or grid points) and  $\mathbf{Y}_2$  ( $n$  observations sites), with the following expressions for the mean and variance:

$$\mu_{\mathbf{Y}} = \begin{bmatrix} \mu_{\mathbf{Y}_1} \\ \mu_{\mathbf{Y}_2} \end{bmatrix} \quad \Sigma_{\mathbf{Y}} = \begin{bmatrix} \Sigma_{\mathbf{Y}_1 \mathbf{Y}_1} & \Sigma_{\mathbf{Y}_1 \mathbf{Y}_2} \\ \Sigma_{\mathbf{Y}_2 \mathbf{Y}_1} & \Sigma_{\mathbf{Y}_2 \mathbf{Y}_2} \end{bmatrix} \quad (5)$$

Then, given a set of observations  $\mathbf{Y}_2 = \mathbf{y}_2$ , a vector of residuals is defined as  $\boldsymbol{\zeta} = \mathbf{y}_2 - \mu_{\mathbf{Y}_2}$ . Thanks to the MVN, it is possible to express the mean and variance of the set of predictions  $\mathbf{Y}_1$ , as follows:

$$\mu_{\mathbf{Y}_1 | \mathbf{y}_2} = \mu_{\mathbf{Y}_1} + \Sigma_{\mathbf{Y}_1 \mathbf{Y}_2} \cdot \Sigma_{\mathbf{Y}_2 \mathbf{Y}_2}^{-1} \cdot \boldsymbol{\zeta} \quad (6)$$

$$\Sigma_{\mathbf{Y}_1 \mathbf{Y}_2 | \mathbf{y}_2} = \Sigma_{\mathbf{Y}_1 \mathbf{Y}_1} - \Sigma_{\mathbf{Y}_1 \mathbf{Y}_2} \cdot \Sigma_{\mathbf{Y}_2 \mathbf{Y}_2}^{-1} \cdot \Sigma_{\mathbf{Y}_2 \mathbf{Y}_1} \quad (7)$$

The initial mean values of  $\mathbf{Y}_1$  are obtained from a GMM, and the variance-covariance matrix is assembled from the standard-deviations associated with the GMM and from the spatial correlation structure of

the ground-motion parameter(s) of interest. Therefore, the results from Eqs. (6) and (7) may be directly used as the updated ground-motion distribution for the generation of the shake-map. Worden et al. [6] also show that this approach enables the consideration of multiple types of ground-motion parameters (e.g., PGA, SA at different periods) simultaneously: thanks to the cross-correlation structure between some ground-motion parameters (esp. spectral responses), it is possible to gain knowledge and constrain shake-maps when only parameters of a given type have been recorded, for instance.

### 2.1.2. Bayesian Network algorithm

In parallel, Gehl et al. [7] have proposed an approach based on the Bayesian updating of correlated Gaussian fields: the prior distribution of the ground-motion field, consisting of a simple predictive scenario of the earthquake event with a GMM, is updated with the observations in order to generate a posterior distribution of the ground motion at each grid point. To this end, a Gaussian Bayesian Network (BN) models the distribution of a given ground-motion parameter  $Y$  at each grid point  $i$  (see Fig. 2). Thanks to the lognormal assumption used in most GMMs, a lognormal-normal conversion is able to express the conditional probability of  $Y_i$  as a normal distribution, with the mean expressed as:

$$\mu_{(Y_i | \mathbf{U}, \mathbf{W})} = X_i + \sigma_{\zeta} \cdot \sum_{j=1}^n t_{ij} \cdot U_j + \sigma_{\eta} \cdot W \quad (8)$$

where  $X_i$  is the mean estimate of the ground-motion parameter from the GMM,  $\sigma_{\zeta}$  is the standard-deviation of the intra-event term, and  $\sigma_{\eta}$  is the standard-deviation of the inter-event term. The matrix of elements  $t_{ij}$  results from the Cholesky decomposition of the correlation matrix between the intra-event terms: spatial correlation models such as the one from Jayaram and Baker [13] may be used to compute this correlation, based on the distances between all grid points and observations. The variables  $U_j$  and  $W$  follow a standard normal distribution and they are essential to model the statistical dependence between the  $Y_i$ , and consequently the updating process.

Observations, either in the form of ground-motion measurements or macroseismic intensities (with the associated uncertainties), are added to the BN as evidence, and then the posterior distribution of the ground-motion parameters is collected at the variables representing the grid points. This approach is able to generate updated maps for the usual ground-motion parameters (i.e., PGA, PGV, SA) as well as macroseismic intensity (see Fig. 3).

The Bayesian updating method has been validated by Gehl et al. [7] on a synthetic case, where the updated ground-motion parameters are shown to be identical to the ‘‘analytical solution’’ (i.e., resolution of a conditional multivariate normal distribution – [11]). This alternative approach has the merit of generating an exact solution for the

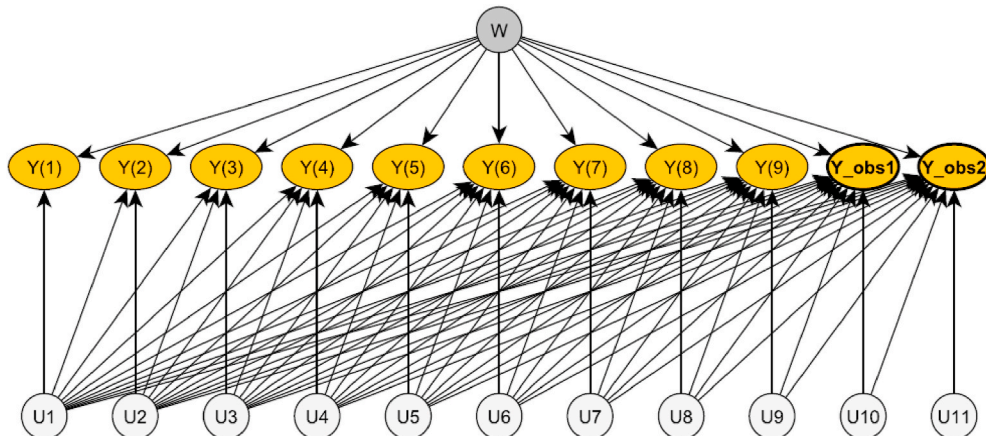


Fig. 2. Illustration of a BN structure for the generation of a shake-map, with nine grid points  $Y(\cdot)$  and two observations  $Y_{obs}$ .

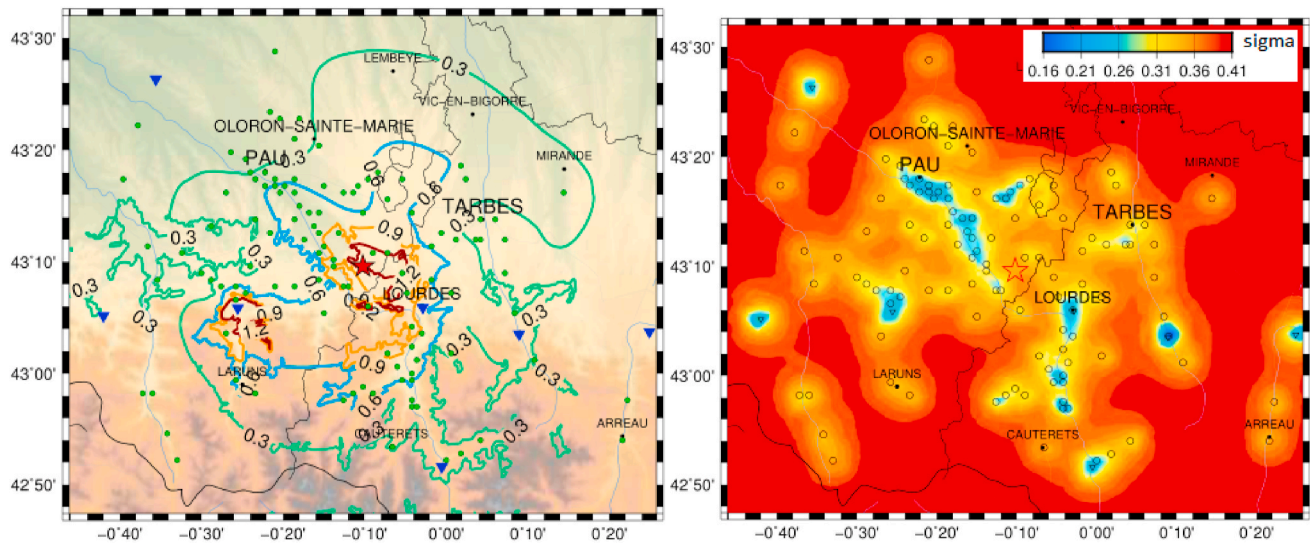


Fig. 3. Shake-map generated with the Bayesian updating approach, for the M 4.3 Lourdes (France) earthquake of December 30th, 2012. Left: contour of PGA (in %); Right: field of associated uncertainty  $\sigma_{\ln PGA}$ . Triangles represent ground-motion measurements and circles are macroseismic observations.

uncertainty field associated with the shake-map, and of being transparent about the treatment of spatial correlation (i.e., direct use of correlation models from the literature). To some extent, it is able to model fields of different ground-motion parameters within the same BN, thus taking advantage of cross-correlation between parameters and potentially improving the precision of the shake-map (similarly to ShakeMap® v4). However, the significant epistemic and aleatory uncertainties related to the choice of GMM and GMICE remain, and the flexibility of BN comes at a higher computational cost than the ShakeMap® v3.5 and v4 methods. Solutions such as the division of the BN into sub-grids have been proposed by Gehl et al. [7]: currently, shake-maps can be processed within a couple of minutes, on the condition that the number of observations to integrate as evidence is not too large (i.e., less than hundreds data points).

### 2.1.3. Alternative ground-motion inference methods

Apart from the above-detailed updating methods, other ways of generating shake-maps have been investigated by Douglas [14]. The methods are classified according to whether they take account of the spatial correlation of the ground-motion field. Among the methods ignoring the spatial correlation of shaking, the following ones are mentioned:

- *Unadjusted GMM accounting for site effects*: it merely consists in the application of a GMM to the parameters of the earthquake event, while adding amplification factors to the soil conditions.
- *Bias-corrected GMM accounting for site effects*: based on the ground-motion measurements, a global bias adjustment is performed on the GMM, in order to account for the actual inter-event variation. This approach is similar to the bias adjustment performed in the ShakeMap® v3.5 algorithm.
- *Derivation of an event-specific GMM*: if there are sufficient ground-motion measurements, a specific GMM with a simple functional form may be regressed from the data, in order to account for both the rate of decay and the inter-event bias.

Two methods accounting for the spatial correction of shaking are also detailed by Douglas [14]:

- *Universal kriging*: it is a geostatistical method that consists of kriging with a drift model, which accounts for data (i.e., the ground-motion measurements) and an underlying trend (i.e., decay with the

epicentral distance). An exponential semi-variogram, with a distance parameter  $a$  (which needs to be defined), is used in order to model the spatial correlation between the observations and the sites of interest.

- *Adapted method of King et al. [15]*: observations are weighted with respect to their distance to the sites of interest, and a GMM is used for correcting differences in epicentral distance (between the sites and the observations).

In Douglas [14], all these methods are tested on ground-motion data from the 2004 Les Saintes earthquake (Guadeloupe, France) and the results are compared to the ones obtained using the ShakeMap® approach. It is found that the more elaborate methods accounting for spatial correlation are associated with lower aleatory variability, and provide similar results in the vicinity of observations. However, at locations that are more than 10 km away from the nearest observation, much larger uncertainties (both aleatory and epistemic) are observed, with little leeway to better constrain the ground-motion field.

Various geostatistical interpolation techniques (e.g., kriging and cokriging methods) have also been benchmarked by Costanzo [16]; in order to derive shake-maps in terms of Arias Intensity and Cumulative Absolute Velocity for the  $M_W$  6.0 Amatrice and the  $M_W$  6.5 Norcia earthquakes, in 2016. A comparison of the author's maps – based on various modelling assumptions – with the official shake-maps published after the two events has led to the identification of current needs for the further improvement of shake-maps: extended regression models between macroseismic intensity and ground-motion parameters, introduction of local site effects, and integration of near-source effects when converting ground-motion parameters to macroseismic intensity.

### 2.1.4. Current challenges and shortcomings

While very straightforward in theory, most shake-map processes require an accurate knowledge of several parameters and models in practice:

- The selected GMM and GMICE have an influence on the distribution of the ground-motion field, and the chosen models should be adapted to the specific area of interest.
- Knowledge of the epicentral parameters of the earthquake (location, depth and magnitude). In particular, the epicentral depth is often poorly constrained with the first automatic notifications

immediately available, while it critically affects the assessment of ground motions in the near field.

- The knowledge of the fault mechanism and dimension is an essential factor as well: in the case of large earthquakes, a fault-source model (instead of a point-source) is required in order to better constrain

near-field ground motions. However, such models may not be defined until several hours following the earthquake event, leading to substantial uncertainties in the earlier versions of the shake-map.

- An accurate map of soil classes, associated to  $V_{s,30}$  values or site amplification factors, is also crucial in order to properly estimate the

**Table 1**

Global information on existing shake-map systems.

Name	Location	Institution(s)	Method	Status	References
<b>Outside Europe</b>					
USGS ShakeMap®	U.S./Worldwide	USGS NEIC	v3.5: Weighted interpolation [10] v4: conditional MVN [6]	Operational	[5,9] <a href="http://earthquake.usgs.gov/data/shakemap">earthquake.usgs.gov/data/shakemap</a>
QuiQuake	Japan	AIST, GSJ	Interpolation from observations by IDW (Inverse Distance Weighted)	Operational	<a href="http://gbank.gsj.jp/QuiQuake">gbank.gsj.jp/QuiQuake</a>
JMA shake-map	Japan	JMA	Generation of an instrumental intensity map	Operational	<a href="http://www.jma.go.jp/en/quake">www.jma.go.jp/en/quake</a> <a href="http://www.data.jma.go.jp/svd/eev/data/suikiei/eventlist.html">www.data.jma.go.jp/svd/eev/data/suikiei/eventlist.html</a>
NTU shake-map	Taiwan	National Taiwan University	Real-time interpolation from a dense network of low-cost accelerometers	Operational	[20]
GeoNet shake-map	New Zealand	GNS Science	Map of Felt Reports	Operational	<a href="http://www.geonet.org.nz/earthquake">www.geonet.org.nz/earthquake</a>
BMKG shake-map	Indonesia	BMKG	ShakeMap® v3.5	Operational	[21] <a href="http://inatews.bmkg.go.id/">http://inatews.bmkg.go.id/</a>
CATnews	Worldwide	CEDIM, Risklayer, EQ Report	Calibration of stochastic scenarios with observations (esp. macroseismic testimonies)	Operational	[22] <a href="https://twitter.com/CATnewsDE">https://twitter.com/CATnewsDE</a>
GA ShakeMap and DYFI	Australia	Geosciences Australia	ShakeMap® v4; DYFI v4	Operational	[23] <a href="https://earthquakes.ga.gov.au/">https://earthquakes.ga.gov.au/</a>
BCSIMS ShakeMap	British Columbia	British Columbia Smart Infrastructure Monitoring System	Custom code based on ShakeMap® v3.5	Operational	<a href="http://www.bcsims.ca/">http://www.bcsims.ca/</a>
KMA ShakeMap	South Korea	Korea Meteorological Agency	ShakeMap® v4, customized	Operational	<a href="http://www.weather.go.kr/XML/INTENSITY/i_3_20190419111643.html">http://www.weather.go.kr/XML/INTENSITY/i_3_20190419111643.html</a>
UAE ShakeMap	Dubai	Dubai Municipality	ShakeMap® v3.5	Operational	[24] <a href="https://shakemap.dm.ae/shake/">https://shakemap.dm.ae/shake/</a>
<b>In Europe</b>					
ShakeMapEU	Euro-Mediterranean area	EMSC, ETH, ORFEUS, EFEHR	ShakeMap® v3.5	Under implementation	[25] <a href="http://shakemap-eu.ethz.ch">shakemap-eu.ethz.ch</a>
SED shake-map	Switzerland	ETH SED	ShakeMap® v3.5	Operational	[26] <a href="http://shakemap.ethz.ch">shakemap.ethz.ch</a>
IPMA shake-map	Portugal	IPMA	ShakeMap® v3.5	Operational	[27] <a href="http://shakemap.ipma.pt/">http://shakemap.ipma.pt/</a>
KOERI shake-map	Turkey (Istanbul)	KOERI, RETMC	Similar to ShakeMap®, or modified Kriging	Operational	[28] <a href="http://www.koeri.boun.edu.tr/sismoatlas2.infp.ro/~shake/shakemap">www.koeri.boun.edu.tr/sismoatlas2.infp.ro/~shake/shakemap</a>
INFP shake-map	Romania	INFP, NIEP	ShakeMap® v.3.5	Operational	[29]
SeisDaRo shake-map	Romania	INFP, NIEP	Custom Matlab code (based on ShakeMap® v.3.5)	Operational	[29]
SisPyr	Pyrenees (France, Spain)	ICGC, OMP, BRGM, IGN, UPC	ShakeMap® v3.5	Operational	[30] <a href="http://www.sispyr.eu/shakemap">www.sispyr.eu/shakemap</a>
POCRISC shake-map	Pyrenees (France, Spain)	ICGC, BRGM	ShakeMap® v4	Under implementation (beta version online)	<a href="https://sismocat.icgc.cat/shakemap/index.php?lang=en">https://sismocat.icgc.cat/shakemap/index.php?lang=en</a>
BCSF shake-map	France (including West Indies oversea territories)	BCSF	ShakeMap® v3.5	Operational	[31] <a href="http://www.franceseisme.fr">www.franceseisme.fr</a>
BCSF shake-map	France	BCSF	ShakeMap® v4	Under implementation	[32]
CASSAT	South-East France	GéoAzur	ShakeMap® v3.5	Operational	<a href="http://sismoazur.oca.eu/">http://sismoazur.oca.eu/</a>
RISVAL-FR	South-East France	GéoAzur	ShakeMap® v4	Under implementation	[33]
IMO shake-map	Iceland	Icelandic Meteorological Office	ShakeMap® v3.2	No longer maintained	<a href="http://hraun.vedur.is/ja/alert/shake">hraun.vedur.is/ja/alert/shake</a>
NOA shake-map	Greece	NOA	ShakeMap® v3.5	Operational	<a href="http://accelnet.gein.noa.gr/shakemaps">accelnet.gein.noa.gr/shakemaps</a>
EPPO-ITSAK shake-map	Greece	EPPO-ITSAK	ShakeMap® v3.5	Operational	<a href="http://shakemaps.itsak.gr">shakemaps.itsak.gr</a>
INGV shake-map	Italy	INGV	ShakeMap® v3.5	Operational	[34] <a href="http://shakemap.rm.ingv.it/shake">shakemap.rm.ingv.it/shake</a>
RSNI shake-map	North-West Italy	RSNI	ShakeMap® v3.5	Operational	<a href="http://www.distav.unige.it/rsni/seismicity.php?lang=en">http://www.distav.unige.it/rsni/seismicity.php?lang=en</a>
RISVAL-IT	North-West Italy	ARPA-Piemonte	ShakeMap® v4	Under implementation	[33]
KNMI shake-map	Groningen (Netherlands)	KNMI	ShakeMap® v3.5	Operational	<a href="http://www.knmi.nl/nederland-nu/seismologie/aardbevingen">www.knmi.nl/nederland-nu/seismologie/aardbevingen</a>

expected level of ground shaking. This is an important source of uncertainty for ShakeMap® 3.5 and the Bayesian inference methods that should not be overlooked, since the amplification coefficients associated with some soil classes can be large. A microzonation of these soil types incorporating a calibration of the amplification factors via geophysical measurements is therefore to be preferred, when possible, over global approaches such as that proposed by Wald and Allen [17].

- Both the GMICE and the site amplification factors that together enable to convert rock accelerations to felt intensities come at the cost of significant additional uncertainties (e.g. the standard deviation related to the GMICE).
- Finally, other parameters of the algorithms pertain to the seismic stations that are to be considered for the computation of the bias (i.e., global level of the shake-map): a selection is usually made based on a cut-off distance from the epicenter (i.e. distant stations are screened out), or on a significant deviation of the observation from the initially GMM estimate. Although already configurable in the ShakeMap® system, the calibration of such choices deserves further investigations.

## 2.2. Current shake-map systems

The USGS ShakeMap® algorithm is applied to the U.S. shake-map system, where specific site amplification models and GMMs are designed for several regional areas (e.g., California, Pacific Northwest, etc.). It also provides a worldwide coverage of most earthquakes, at the cost of sometimes simplified models that must cope with a paucity of detailed data in some locations. For instance, the estimation of soil amplification factors from the topographic slope [17] constitutes a very convenient solution for first-order estimates, although its accuracy in less seismically active areas remains subject to debate [18]. Hybrid solutions such as the one proposed by Heath et al. [19] also enables to refine soil amplification factors by including regional maps. Thanks to the operational readiness of the ShakeMap® package, it has been re-used and set up by several national or regional institutions worldwide (e.g., Switzerland, Italy, Greece, France, Romania, etc.): the algorithm remains the same, and local users have the possibility to exploit their own specific models and data streams (e.g., site amplification data, GMMs, GMICE, sources of observations, etc.), thus ensuring a great flexibility of the ShakeMap® tool.

Recently, the USGS ShakeMap® system has been upgraded from

version 3.5 to version 4: one of the main changes pertains to the application of the “MVN approach” [6], i.e. the modelling of the ground-motion field through a conditional multi-variate normal distribution. This technique has the merit of removing “abrupt islands” close to the observations (due to the “radius of influence” in the former interpolation scheme) and of providing a much smoother field of uncertainty. However, most worldwide declinations of the ShakeMap® system are still operating with the former version 3.5, and it is expected that the version upgrade might take several months or years in most countries. A non-exhaustive list of the most common shake-map systems is described in Table 1.

For some of the selected shake-map systems, Table 2 provides further details on the sources of real-time data that are exploited: the characteristics of the earthquake event after its detection, the seismic networks that provide the ground-motion measurements, and the source of the macroseismic testimonies. Although it is technically possible in most algorithms, the integration of macroseismic intensities is not systematic in all systems: due to the dense coverage of seismic stations, shake-maps in Japan rely only on ground-motion measurements, which are directly converted into the JMA instrumental intensity [35]. It is worth noting that the collection of macroseismic intensities suffers from a lack of harmonized procedures between the different systems, with different types of online forms and possibly different interpretations of the accounts into a macroseismic scale [36].

Finally, the site amplification models for the different shake-map systems are detailed in Table 3. National coverage in terms of soil classes or  $V_{s,30}$  ranges is often not currently available. For now, local shake-map systems are more susceptible to benefit from an accurate soil classification, which is easier to generate over a small area (e.g., Pyrenees in France, Groningen area in the Netherlands).

## 3. Rapid loss assessment systems

Structural damage and loss assessment software in an earthquake rapid response context need to be quick enough to deliver first estimates, and they should be able to cover potentially large built areas. The following section presents the main types of damage and loss assessment algorithms, and the current modules and systems in which they are used.

### 3.1. Damage assessment algorithms

There are several types of damage assessment algorithms, as

**Table 2**  
Sources of real-time data for selected shake-map systems.

Name	Earthquake parameters	Measured ground motions	Macroseismic observations
USGS ShakeMap®	NEIC	ANSS (accelerometers & broadband)	Did You Feel It? <a href="https://earthquake.usgs.gov/dyfi">https://earthquake.usgs.gov/dyfi</a>
JMA shake-map QuiQuake	JMA –	JMA network (seismographs + seismic intensity meters) + NIED data NIED networks: K-NET (strong-motion accelerometers) and KiK-net (strong motion seismometers in boreholes)	–
SED shake-map	SED-data processing hubs from ETH	CHNet (SDSNet→ Streckeisen STS-2 broadband seismometers & SSMNet → broadband 200Hz accelerometer)	Seismo.ethz: Did You Feel an Earthquake?
KOERI shake-map	KOERI	KOERI, RETMC – Broadband (BB), Accelerometer (SM), Short-period (SP) seismometers	–
INFP shake-map SisPyr	NIEP ICGC, IGN, OMP, BRGM	Romanian Seismic Network (accelerometers) ICGC, IGN, OMP, BRGM (BB and accelerometers)	– BCSF online questionnaire: <a href="http://franceseisme.fr/formulaire">franceseisme.fr/formulaire</a>
BCSF shake-map	Detection by CEA/LDG	RESIF network (accelerometers)	BCSF online questionnaire: <a href="http://franceseisme.fr/formulaire">franceseisme.fr/formulaire</a>
RISVAL-FR	GéoAzur	RESIF network (accelerometers)	BCSF online questionnaire: <a href="http://franceseisme.fr/formulaire">franceseisme.fr/formulaire</a>
RISVAL-IT	ARPA-Piemonte	Regional Seismic network of Northwestern Italy	–
NOA shake-map	NOA	Hellenic Unified Seismological Network-HUSN	<a href="http://noa.gr/did-you-feel-it/">noa.gr/did-you-feel-it/</a>
EPPO-ITSAK shake-map	ITSAK	Permanent strong motion instruments + mobile accelerometers	–
INGV shake-map	INGV-Roma	RAN network (accelerometers)	Haisentidoil terremoto.it (=DYFI)
KNMI shake-map	KNMI	Netherlands Seismic and Acoustic Network, Groningen seismic network (accelerometers)	–

**Table 3**  
Modelling and processing parameters for selected shake-map systems.

Name	Site amplification model
ShakeMap®	Global $V_{s,30}$ Hybrid Map [19]
JMA shake-map	Amplification factors derived from Japanese $V_{s,30}$ map (geomorphologic + geological features)
QuiQuake	Amplification factors derived from Japanese $V_{s,30}$ map (geomorphologic + geological features)
SED shake-map	Amplification factors based on macroseismic intensity increments
KOERI shake-map	$V_{s,30}$ map for metropolitan Istanbul (from microzonation project; geology + topography)
INFP shake-map	Estimation of $V_{s,30}$ based on topographic slope [17]
SisPyr	Regional map of EC8 soil classes (converted to amplification factors) – [37]
BSCF shake-map	Estimation of $V_{s,30}$ based on topographic slope [17]
RISVAL-FR	Estimation of $V_{s,30}$ based on topographic slope [17], with integration of microzonation of Nice city area [38]
RISVAL-IT	Default factors from Borcherdt [39]; testing factors calibrated for the area and with different velocity ranges for soil classification.
NOA shake-map	Estimation of $V_{s,30}$ based on topographic slope [17]
EPPO-ITSAK shake-map	Estimation of $V_{s,30}$ based on topographic slope [17]
INGV shake-map	Amplification factors obtained from $V_{s,30}$ , using a map of EC8 soil classes
KNMI shake-map	Amplification factors computed with zone-specific coefficients. The area around the gas field has been categorized in >100 zones, using a $V_{s,800}$ model, since the top 800 m consists of unconsolidated sediments.

detailed in Calvi et al. [40]. Some of them are based on empirical methods, others on analytical methods that involve mechanical considerations, and finally they can be hybrid and built on a combination of analytical and empirical basis. The paragraphs below list the main algorithm types.

### 3.1.1. Assessment of damage to buildings and infrastructure components

First, the Damage Probability Matrices (DPM) initially proposed by Whitman et al. [41] express how likely a discrete level of ground-motion intensity is to generate a given level of damage. The likelihoods are reported in the form of tables crossing the discrete ground-motion and damage levels.

The Vulnerability Index Method (e.g. Ref. [42]) uses various building characteristics affecting its stability (e.g. state of conservation, type of materials, floor configuration), it assigns a qualification coefficient to them (from optimal to unfavourable), weighted by the relative importance of the criterion, and it eventually returns a global index reflecting the building vulnerability. This methods relies mostly on expert judgement [40].

Others methods are based on continuous Vulnerability Curves (VCs), which represent an improvement compared to the discrete levels considered in the DPMs. VCs relate a ground-motion parameter (PGA, macroseismic intensity or sometimes spectral acceleration or displacements) to the probability of reaching a given damage state (D1 to D5 in the MSK scale, [43]).

Although the aforementioned methods are mostly empirically derived, some part of the DPMs can sometimes make use of non-linear dynamic models of different building classes [44] for instance, and computer simulations can also be used to complete vulnerability functions [45]. Such methods can be qualified as “hybrid”.

On the analytical side, we can distinguish three main types of methods: collapse mechanism based, capacity spectrum based and fully-displacement based.

The collapse mechanism based methods use so-called collapse multipliers to evaluate if a structure will collapse, based on mechanical principles. VULNUS [46] and FaMIVE [47] are two examples of these methods.

Capacity Spectrum Methods [48] rather examine the deformation of

a building subject to increasing lateral forces (pushover curve). Ground motion is characterized by spectral response, generally based on a standard spectrum shape. The spatial distribution of ground motion can be determined using either deterministic ground motion analysis, probabilistic ground motion maps or user-supplied maps. The elastic response spectrum is reduced in order to consider the non-linear behaviour of the (hysteretic energy dissipated by) buildings when it goes beyond their elastic limits. Different methods can be used for reducing the elastic response spectrum, mostly based on two principles: (i) the use of overdamped elastic spectrum in Freeman’s approach obtained via an additional equivalent viscous damping ratio related to the hysteretic capacity of the system or (ii) the use the inelastic spectra in Fajfar’s approach obtained via the behaviour factor which is based on the ductility of the structure. Generally, an iterative procedure is implemented for determining the performance point, in order to ensure the compatibility between the reduced demand spectrum with the capacity spectrum, and the level of non-linearity of the structure.

The last methods are the fully Displacement-Based methods [49]. In the latter, only the comparison between displacement capacity and displacement demand is considered.

Most of the current modules able to perform damage estimation have been reviewed in Erdik et al. [8] and in Makhoul and Argyroudis [50]; a software inventory that comprises the characteristics of around 50 packages. Here, we list the most common tools that enable the use of ground motion estimates and of exposure and vulnerability maps in order to assess the level of damage and loss at different levels of resolution. They have originally been developed for the computation of prospective damage scenarios at city, regional or national scale in preparedness and mitigation phases; therefore, their application is suitable for near-real-time computations in a RRE context.

ELER’s routine [28] is a capacity spectrum based method that performs loss estimation (building damage, casualties, economic loss), and that uses building inventories (type, height and year) for the vulnerability assessment. At a high-resolution level, the damage on buildings and associated uncertainties are evaluated using spectral displacement-based analytical vulnerability relationships [51].

SELENA [52], is another capacity spectrum based method, where the vulnerability is assessed based on the spectral parameters (accelerations and displacements), and the ground motion estimates are provided using deterministic or probabilistic analysis, including site-effects. The uncertainties may be computed via a logic-tree and a Monte Carlo approach.

In DBELA (Displacement Based Earthquake Loss Assessment [53], and SP-BELA (Simplified Pushover-Based Earthquake Loss Assessment - [54]), the vulnerability of the building is determined based on mechanical principles. While DBELA is a fully displacement-based method, SP-BELA uses a simplified technique in order to reduce the computational cost. It has been implemented essentially in regions with European/Mediterranean types of buildings.

We also mention here the Armagedom software [55], which follows the RISK-UE methodology [56], and uses a mix of the methods discussed above to perform loss assessment. The building typology is inspired by the EMS-98 classes as defined in Grunthal [57]; and refined with sub-typologies. The basic analysis level is an empirical method (namely LM1 in RISK-UE) and is derived from the work of Giovinazzi and Lagomarsino [58]; where vulnerability indices are assigned to the different building types. The second analysis level (LM2) is an analytical method similar to HAZUS 99 [59], where each building class is assigned a capacity curve. The performance of the building in response to the seismic demand is then assessed using the capacity spectrum method.

Lestuzzi et al. [60] applied the RISK-UE methodology (both the empirical method LM1 and the mechanical method LM2) to the building stock of two cities, namely Sion and Martigny, located within the highest seismic zone of Switzerland. They conclude that for qualitative analysis, both methods are able to identify the most vulnerable parts of a city, as well as which one is most vulnerable among a group of investigated



cities. They discuss the pros and cons of each level and recommend carefully interpreting the quantitative results for both levels.

Finally, the OpenQuake platform [61] - [www.globalquakemodel.org/openquake](http://www.globalquakemodel.org/openquake)), which has been developed from an initiative of the Global Earthquake Model (GEM), provides a free, open-source software for the assessment of earthquake hazard and risk. OpenQuake contains an integrated hazard module, which can perform a wide range of computations (e.g., probabilistic hazard assessment, earthquake scenarios, seismic source disaggregation) along with the treatment of uncertainties via logic trees. Similarly, the risk module offers a variety of features, such as scenario-based damage/risk assessment, classical probabilistic damage/risk analysis or stochastic event-based damage/risk analysis. Inputs for the damage assessment step consist in exposure models (i.e., GEM building taxonomy) in terms of built areas or single assets. Fragility models are then applied in order to estimate damage distribution. In the end, vulnerability functions may also be applied in order to provide various types of loss measures (e.g., replacement costs, casualties, etc.).

### 3.1.2. Assessment of human losses

Experience shows that after destructive earthquakes, it often takes many hours, or even days, to gain a realistic view of the overall magnitude of human tolls [62]. With a disaster management point of view, the indicators related to human losses are therefore particularly useful during the first hours after the occurrence of an earthquake, because they can allow a better dimensioning and a better allocation of resources for search and rescue activities, as well as for assistance to the population. Unfortunately, relatively little work has been devoted to the issue of estimating human impacts to date, and the models used often lack high-quality data for calibration. Using the classification proposed by Maqsood and Schwarz [63]; methodologies for human losses assessment can be classified into five levels of increasing complexity:

- Level 1: empirical definition of loss rate as a function of an IM value (e.g., PAGER empirical model - [64]);
- Level 2: improvement of level 1 by taking into account the building stock by rough typologies, and the resident population (e.g., PAGER semi-empirical model - [65]);
- Level 3: taking into account the levels of expected damage to buildings, and empirical losses rates [66];
- Level 4: improvement of level 3 by taking into account the structural vulnerability of the building stock (e.g., PAGER analytical model - [67]; HAZUS - [59]);
- Level 5: improvement of level 4 by taking into account temporal variations in the exposure of populations.

From level 3 and upwards, it is possible to use the results of the building damage assessment models (see Section 3.1.1) to deduce probable human losses associated to the level of physical damage to structures and to the occupation of buildings, for example by using a casualties matrix such as the one proposed by Coburn and Spence [68]. Spence [69] has also updated the previous casualties matrix by proposing injury distributions for specific building types. Note that while linear models are the most used methods for assessing feature correlation, Jia et al. [70] recently proposed an integrated ensemble model established using deep-learning techniques, by considering nine different predictive features.

Other models offer a much more detailed consideration of possible human losses as a function of their position within buildings and their actual exposure to failures of structural elements [71]. However, applicability of such models to RREs systems remains challenging, because it requires a very refined modeling of the damages at the scale of each building considered individually, and not statistically at the scale of building blocks.

Due to the many parameters that can directly influence the amount of human losses during an earthquake, the level of uncertainty on the predicted values is therefore high. With the notable exception of the

study by Gobbato et al. [72]; very little work has been devoted to quantifying this uncertainty. However, it appears that one of the main avenues for improvement that can reduce this level of uncertainty is the development of level 5 models, explicitly taking into account the spatio-temporal modulations of population exposure, in, near and outside buildings.

## 3.2. RRE systems providing loss estimates

This section details some of the current systems for the estimation of damage and losses in a RRE context. First, common software that are able to perform rapid damage computations, through mechanical or empirical approaches, are briefly described. Then, the various existing RRE systems are discussed: a distinction is made between those that propose a direct and automated link between the shake-maps and a damage or loss estimation software, and those that rely on alternative approaches. A summary of the rapid damage and loss assessment systems is proposed in Table 4, and illustrated in Fig. 4, with the required input data and the output format of each system.

### 3.2.1. RRE systems directly based on shake-maps

The following sub-sections provide a more detailed description of some of the most common RRE systems that use near real-time shake-maps as inputs.

**3.2.1.1. USGS PAGER system.** The PAGER (Prompt Assessment of Global Earthquakes for Response) system developed by the USGS constitutes a prime example of robust tools used for loss and damage estimation [73,74]. Immediately following the earthquake, updated ground-motions maps are provided by the USGS ShakeMap® system. They can then be combined with vulnerability assessment for loss estimation. Global population databases provide the amount of people exposed to a given macroseismic intensity level, leading to the estimation of potential casualties and economic losses thanks to country-specific vulnerability and loss models [74]. The approach is empirical in developing regions having experienced an important number of damaging events. In highly developed countries, strong building codes and inventories enable the use of analytical methods, and semi-empirical solutions exist for regions corresponding to a mix of these end-members.

The use of global databases and models makes the PAGER system applicable worldwide, while its automated and fast execution is crucial for a timely sizing of the event and a triggering of appropriate response protocols. Like-country groups are used for the countries without loss data from past events. It does not use regional models as they tend not to be calibrated, particularly for fatalities which requires building inventories, collapse fragilities, occupancy and fatality rates to be approximately correct. Loss estimates are only based on empirical models while other estimates such as the distribution of impacted buildings make use of the other methods.

**3.2.1.2. USGS ShakeCast system.** ShakeCast (ShakeMap Broadcast: <http://usgs.github.io/shakecast> - [75]) is another similar fully-automated open-source system using ShakeMap® input, and HAZUS methodology [59]. Although HAZUS is the default methodology, the user can also specify the input such as fragility curves for buildings, bridges, etc. Shake-maps are applied to a list of critical and industrial facilities, for which a probability of damage is estimated through fragility curves. Alerts are broadcasted on a web interface, and sent by emails and texts to registered end-users, in order to be used for prioritizing inspection (green, yellow, orange or red).

**3.2.1.3. GDACS.** The PAGER tool providing casualties estimates is included in more general alert systems such as the Global Disaster Alert and Coordination System, GDACS ([www.gdacs.org](http://www.gdacs.org)). GDACS is a

**Table 4**  
Input data and expected outputs for the studied loss assessment systems.

Loss estimation system	Input data	Output	Scale	Operationally & Output status
PAGER	Shake-map + empirical or analytical vulnerability assessment	Fatalities & economic losses estimates + user-friendly depiction of uncertainties	- Population exposed at each intensity level - At the level of the whole event	- Operational as a service - Public
ShakeCast	Shake-map + facility inventory	Shaking values and inspection priorities. Email/text alerts	At the level of individual facilities	- Operational as a service - Restricted to registered users (e.g., infrastructure managers)
GDACS	PAGER output	Three-level color alert	At the level of the whole event	- Operational as a service - Public
SeisDaRo	Custom shake-map + building inventory + vulnerability data	Fatalities graphs and exposure tables. Fast global damage estimates + more accurate analysis of fatalities due to building collapse.	At the level of cities/municipalities	- Operational as a service/demonstrator - Restricted to authorized users
Istanbul ELER	Shake-map + building inventory database + occupancy/population database	Damage and loss maps	At the level of a city district/large building block	- Operational as a service/demonstrator - Restricted to authorized users
SEISAID	Shake-map + building inventory database + occupancy/population database	Collapsed dwellings, and injuries	At the level of the whole event, and disaggregation at the municipality level	- Operational as a service/demonstrator - Restricted to authorized users
QLARM	Scenario earthquake + empirical relations	Fatalities and average damage on buildings on global scale	- Exposure of each population settlement - Grade for the whole event	- Operational as a service - Public
SIGE-DPC	Earthquake characteristics + empirical relations	Collapsed dwellings, unusable dwellings, fatalities and homeless.	At the level of cities/municipalities	- Operational as a service - Restricted to Italian civil protection
EQIA (ESMC)	Earthquake characteristics + population density (LandScan)	Global impact estimate (range)	At the level of the whole event	- Under development & test
TELES	Earthquake scenario + liquefaction effects	Damage maps and tables	At the level of a city district	?
READY	Intensity map	Damages on roads and buildings, inaccessible roads	At the level of a city district/large building block	?
SUPREME	Spectral intensity	Damage on gas pipes/automatic shut-down	At the level of facilities (buried pipelines)	- Operational as a service - Restricted to gas line operators
Earthquake-Report	Intensity maps, online news	Injuries, fatalities, evacuations	At the level of the whole event	- Public webpage activated for large and damaging events
ISARD	Earthquake characteristics + empirical relations	Collapsed dwellings, unusable dwellings, fatalities and homeless.	At the level of cities/municipalities	- Operational as a service - Restricted to Catalan civil protection

cooperative framework between the United Nation and the European Union comprising and gathering the data and tools from several organizations: JRC (Joint Research Center of the European Commission) & INFORM (Index for Risk Management), NEIC (National Earthquake Information Center) & USGS, OCHA (UN Office of Coordination of Humanitarian Affairs), and INGV. Every 5 min, the data (earthquake magnitude, depth, location, population within 100 km, vulnerability) is obtained via web services, and a qualitative three-level alert is issued (green, orange or red), depending on the extent of the event (earthquake or other natural hazard) and the ability of the country to cope with it.

**3.2.1.4. SeisDaRo.** In Romania, SeisDaRo 3 [29] is a near-real-time system based on the PAGER methodology and the SELENA module. It is directly connected to a custom shake-map system (based on the ShakeMap® v3.5 approach) and it can deliver loss maps by running all of the system's modules in less than 6 min. First, global loss statistics from the event are generated from the PAGER methodology. Then, within a few minutes, a more detailed account of the earthquake's impact is made available, using the SELENA algorithm to estimate damages and losses.

**3.2.1.5. ELER.** Operational in the Istanbul area, this system [28] uses the shake-maps generated by KOERI/RETMC, which are available within a few minutes after the event. The calculations of damage and loss are then performed on a grid using, in addition to the shake-map, exposure and vulnerability data. The grid-based building inventory

was first compiled by using the year 2000 Turkish Statistical Institute (TUIK) Building Census (including information on the construction year, number of floors, and building construction type and the demographic data). In a second step of the project, a district-based building inventory of Istanbul was performed to complete the TUIK statistics and the final inventory was finalized into 0.005° grids by using 2008 building line geometries of 1/1000-scaled existing maps. The building damage is evaluated using the ELER methodology, and the loss estimation with the HAZUS-MH methodology [59].

**3.2.1.6. SEISAID.** In France, BRGM (French Geological Survey) has developed a rapid response system based on the PAGER approach [76, 77]. Implemented in the whole French mainland territory, the SEISAID tool generates rapid shaking estimates and it projects population density data on seismic intensity levels, similarly to the PAGER approach. It permits to rapidly estimate the number of casualties and homeless people. Data from past French earthquakes and from most seismic scenarios have been used to calibrate the relation between the macro-seismic intensity and the human losses. Currently, BRGM is upgrading the SEISAID system by automatically connecting the shake-map outputs to the Armagedom software, in order to generate more accurate damage and loss scenarios in areas where vulnerability data is available.

Four versions are currently being finalized:

- Two "research driven" demonstrators [78]: one in the Pyrenean cross-border area between France, Spain and Andorra, and the other

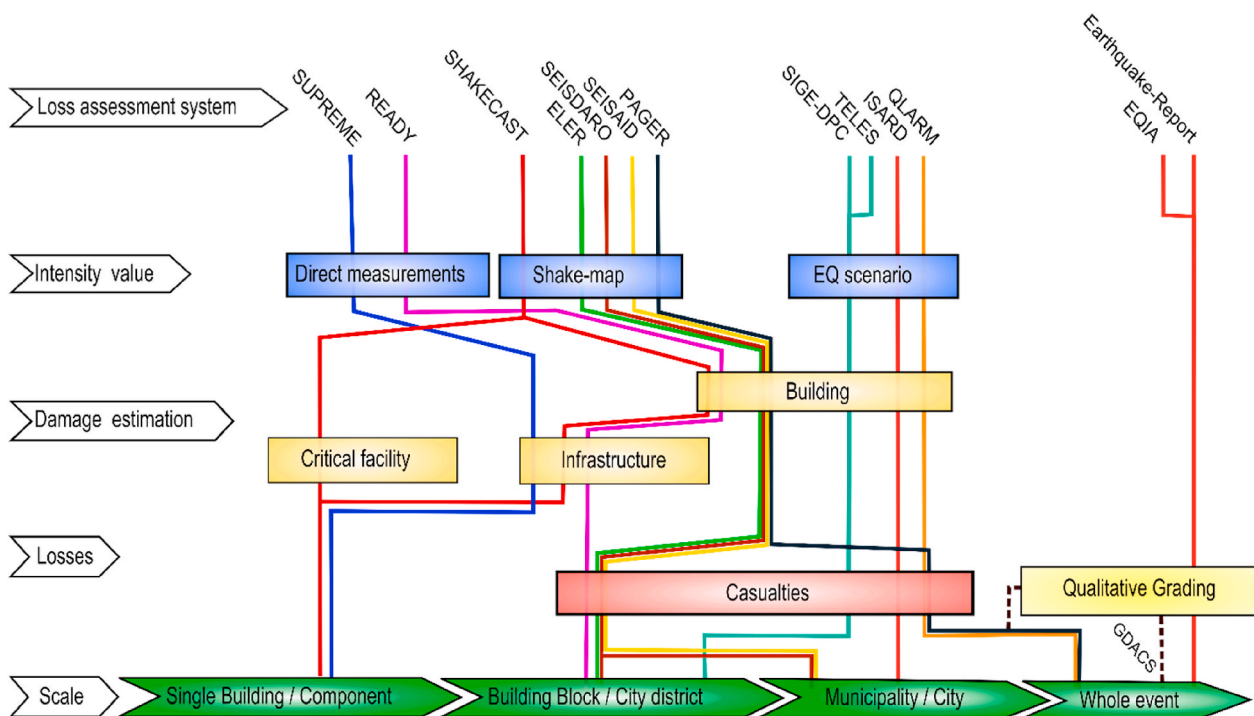


Fig. 4. Summary of the selected damage and loss assessment systems characteristics.

in Southeast of France [33], which rely on a web service which, upon receipt of a shake-map, performs a rapid loss assessment, and delivers the results in PDF reports.

- Two “user driven” pre-operational systems ordered by the French authorities: one for the island of Mayotte (French overseas territory located in the Indian Ocean) and the other for the French West-Indies (French overseas territories located in the Pacific Ocean, including the islands of Martinique, Guadeloupe, Saint-Martin and Saint-Barthélemy). Already implemented since October 2019, the SEISAid-Mayotte system couples the creation of a Bayesian shake-map [7] with the Armagedom loss assessment code. The results (i.e., number of casualties and injured people, and number of partially or totally collapsed buildings, at the scale of a municipality) are intended to be communicated via e-mail to civil protection services, a few minutes after the earthquake event.

### 3.2.2. RRE systems not based on shake-maps

In contrast with the above-detailed systems, the following subsections describe tools that do not directly rely on the outcomes of the shake-map systems: either they use specific earthquake scenarios without accounting for field observations or they directly estimate losses from the earthquake’s characteristics.

**3.2.2.1. QLARM.** ICES Foundation (<http://www.icesfoundation.org/Pages/qlarmEventList.aspx>) provides loss estimates within less than 24 h after a potentially damaging earthquake worldwide. This is done in partnership with the Swiss Seismological Service and eventually provides alert levels with the number of fatalities and the average damage of buildings. The software used is called QLARM for earthquake Loss Assessment Response [79]. The ground shaking is estimated for each population settlement using the earthquake characteristics and a  $V_{s,30}$  map (based on the topography). The damage estimation is obtained using empirical relations derived from ~1000 earthquakes for which the losses were known. The percentage of population belonging to classes of vulnerability (definition of the classes based on the building type) is evaluated. The distribution of the population depending on the time of the event is also taken into account. The results are the percentage of

buildings in each of the five defined damage states, as well as the number of fatalities and injured people in each settlement. Results are available on the ICES Foundation website, and they are automatically sent to the subscribers of the QLARM system.

**3.2.2.2. SIGE-DPC.** In Italy, an automatic procedure (SIGE - Information System for Emergency Management), activated by the Department of Civil Protection (DPC), uses the early characteristics of the earthquake event in order to estimate an expected distribution of structural damage and human casualties [80]: however, interestingly, it appears that the shake-map step is bypassed, with no immediate use of measured or observed ground shaking in order to update intensity maps.

On the other hand, web-based GIS tools have been developed at EUCENTRE (European Centre for Training and Research in Earthquake Engineering) for the Italian DPC: they are aimed at developing near-real time damage scenarios for a wide range of exposed assets and systems, such as residential buildings [81], schools [82,83], port infrastructure [84], road networks [85] or airports [86].

**3.2.2.3. Earthquake Qualitative Impact Assessment (EQIA).** EMSC (Euro-Med Seismological Centre) has developed EQIA, an Earthquake Qualitative Impact Assessment [87], which provides fast and automatic impact assessment for worldwide crustal earthquakes, with a magnitude 5 or higher. It provides a range of potential impacts (based on intervals of potential fatalities), in order to rate the severity of the event for the triggering of rapid actions. To this end, two empirical equations are used: a GMM for the estimation of the impacted area, and an equation relating the number of fatalities to the earthquake magnitude and to the population density. This approach has the merit of bypassing the shake-map step and of providing a direct impact estimate with a little amount of input data. For large earthquakes of magnitude 7 or higher, the source is modelled as a 1D finite rupture, and different assumptions regarding the position of the fault and its nodal plane are taken into account, adding up to the uncertainties of the earthquake scenario. A comparative study by Julien-Laferrière [88]; between EQIA predictions on past earthquakes and actual impacts, reveals a satisfying performance by EQIA. Currently, EQIA outcomes are not made publicly available,

however they are communicated to a group of selected end-users or when prompted by governmental organizations (e.g., French civil protection).

**3.2.2.4. The TELES system.** The Taiwanese system TELES (Taiwan Earthquake Loss Estimation System – [89]) is based on the HAZUS methodology, and it provides decision support after strong earthquakes. The earthquake data comes from the Central Weather Bureau networks and the parameters (location, magnitude) are given by TREIRS (Taiwan Rapid Earthquake Information Release System) within 90s after the event. This enables to estimate the ground motion (PGA and PGV) from a scenario earthquake and prediction equations. The liquefaction effects are included in the method and a probability of damage state for 15 different types of buildings is given, using analytical methods. Damage maps and tables are automatically generated within three to 5 min after receiving the earthquake alert. For now, this procedure does not seem to integrate the new Taiwanese shake-map system yet.

**3.2.2.5. Japanese systems READY and SUPREME.** Two other systems exist in Japan: the READY system [90], and the more specific SUPREME system [91], for possible damages on gas infrastructures. READY has an associated array of strong motion accelerometers and borehole systems for liquefaction monitoring. The stations are connected to observation centers via high-speed telephone lines and satellites as a backup. The intensity map is immediately issued, along with other useful information such as hospital or shelter locations. Thanks to an agreement with civil construction firms, the damage of road structures and transportation conditions can also be rapidly assessed. The SUPREME system uses Spectrum Intensity Sensors in order to evaluate damages on gas pipes. The response spectra are evaluated in the range 0.1–2.5s, and if the spectral intensity becomes greater than 30–40 cm/s the decision to shut down the gas supply is made.

**3.2.2.6. ISARD system.** Resulting from a cross-border project between France, Spain and the principality of Andorra, and followed by the SISPyR project ([www.sispyr.eu](http://www.sispyr.eu)), the ISARD system (Goula et al. [92]) has been used in operational mode since 2007 by the civil protection of Catalonia, Spain). Operated by the ICGC (regional geological survey of Catalonia), this system performs rapid loss assessment by coupling a rough estimate of the seismic intensity using an Intensity Prediction Equation (IPE), with a loss model similar to that described by Sedan et al. [55]. The result is sent in less than 10 min by SMS to an on-call seismologist in charge of its validation, then of sending reports to civil protection via SMS and e-mails.

### 3.3. Summary of rapid loss estimate systems

A summary of the rapid damage and loss assessment systems is proposed in Table 4, with the required input data and the output format of each system. Fig. 4 provides a visual representation of the different systems characteristics.

## 4. Discussion and suggested advances

The above review has highlighted several noteworthy points and issues related to the implementation of shake-maps and rapid loss assessment systems worldwide, and especially in Europe. We can formulate the following observations with respect to modelling data and real-time inputs in shake-maps:

- For the near real-time generation of shake-maps (i.e., within minutes of the event), it is currently difficult to get an accurate knowledge of the faulting mechanism or of the fault geometry. First-order approximations usually consist in the adoption of a faulting style that is consistent with the seismo-tectonic context of the cover area.

ShakeMap® uses the rapid moment tensor if available, or a composite mechanism taking into account the location and depth of the hypocenter in the meantime (if enough stations record the event, such as around California cities, then mechanism, site, path and even finiteness are included implicitly in the data). In addition, empirical relations may also be used to assume fault dimensions from the earthquake magnitude [93], in order to estimate distance metrics such as Joyner-Boore distance or distance-to-rupture (ShakeMap® v4 uses the point source approximation from Thompson and Worden [94]). Alternatively, the Earthquake Qualitative Impact Assessment by EMSC proposes to integrate these uncertainties on the source characterization by considering several extreme fault configurations, in order to apply confidence bounds around the results. This approach is already implemented in ShakeMap® v3.5 and v4 algorithms, and the uncertainties associated with the source approximation are propagated and associated to each IM of the grid. This should also be implemented in the Bayesian approach of Gehl et al. [7]; especially in the case of large earthquake with an extended source. We note that in the case where the fault geometry data is available like in California (first-order fault model), the ShakeMap® system is well suited to account for the geometry and optionally for the directivity. One of the implemented methods to include directivity is based on Rowshandel [95]. Convertito et al. [96] also presented a Bayesian approach for including in near-real time the directivity in shake-maps, however it is not currently implemented in the software.

- Another source of uncertainty lies in the characterization of site amplification factors: by default, most shake-map systems use the Wald and Allen [17] model based on topographic slope. While this is better than no amplification map at all, and while the influence of amplification factors on the result decreases with increasing ground-motion and or intensity data, there is no guarantee that it provides accurate results for the area of interest. Therefore, regional maps should be used when available, to complement or replace estimated  $V_{S,30}$  values from topographic data, using the method of Heath et al. [19] for instance. Moreover, a proper characterization of the sites where ground motions are recorded is crucial, since inaccurate amplification factors may propagate errors when devolving the observations to rock conditions and, in turn, they may alter the whole shake-map field (this is a less important problem in ShakeMap® v4 where the observations are not converted down to rock condition before interpolation). Therefore, recent efforts carried out in the SERA project for a better characterization of site conditions in Europe should be integrated in the upcoming developments.
- The choice of the GMM models to be used in the shake-maps is also very disparate between the different systems, due to the lack of *ad-hoc* equations for most areas in Europe. A solution is to generate shake-maps with a logic tree of GMMs (i.e., as in probabilistic seismic hazard analyses) using tools such as GEM (Global Earthquake Model) OpenQuake library of GMMs [97], in order to integrate the epistemic uncertainty due to GMM selection. Using these tools provided by OpenQuake, ShakeMap® packages allow any user to weight a suite of GMMs according to the regional PSHA logic tree [98,99], integrating the errors which can be propagated to the loss and damage assessment [100]. It can also be done with the Bayesian updating method, although this comes at the expense of longer computation times and added complexity to the final outcome. It is worth noting that most shake-map algorithms adjust the global level, by correcting the bias (ShakeMap® v3.5) or by updating the inter-event error term (ShakeMap® v4.0 and method by Ref. [7]), so that the influence of the GMM on the global level of the updated ground-motion field may be limited: only local differences, due to different decay rates and differences in the treatment of site amplification, may remain.
- The integration of macroseismic testimonies is not systematic in all shake-map systems, with various ways of collecting and interpreting the data (i.e., different types of online forms). The duration required

to collect meaningful data and to translate it into macroseismic values constitutes a challenge for their use in near real-time applications. For instance, the uncertainty treatment of macroseismic testimonies is formalized by Worden et al. [6]: they are given default uncertainties (i.e., a nugget term) and *DYFI* data have uncertainties inversely related to the number of reports in a 1x1-km grid. Less conventional sources of social data, such as the use of the mobile applications (LastQuake - [101]; Earthquake Network - [102] or the data mining of social media (e.g., Twitter feeds - [78]), have proven to be very efficient thanks to the reactivity of users right after an earthquake event (i.e., a few seconds to a few minutes). Their use as additional data inputs for shake-maps is worth investigating, in order to cover the time gap before the arrival of more accurate macroseismic intensities (i.e., after several minutes).

In terms of shake-map algorithms, the version 4.0 of ShakeMap® offers substantial improvements over the version 3.5. The weighted interpolation algorithm, which is based on the definition of “radii of influence” that are difficult to quantify in practice, is replaced by a matrix-based procedure that relies on the multi-variate normal (MVN) distribution. The latter approach presents the benefit of generating exact solutions of the updated ground-motion field, with an accurate uncertainty structure [6]. Moreover, this approach is able to consider multiple types of IMs, for instance by accounting for the statistical cross-correlation between spectral ordinates at various periods: this feature is especially useful when dealing with inter-connected exposed assets that are susceptible to various types of IMs (i.e., loss assessment of infrastructure systems). In parallel, the Bayesian updating approach by Gehl et al. [7] is based on the theory of spatially correlated Gaussian fields, in order to update the ground-motion field from various types of observations. The Bayesian approach is based on the same mathematical concepts as the procedure by Worden et al. [6]; so that the results are identical when the same assumptions are used. It is also able to handle cross-correlation between different IMs, although at the cost of longer computation times. Regardless of the approach used, it should be noted that these two recommended procedures provide an accurate description of the uncertainties associated with the updated ground-motion field, so that these uncertainties should ideally be propagated to the loss assessment step.

Finally, additional comments and recommendations can be made on existing rapid loss assessment tools:

- Some systems, such as PAGER, GDACS or EQIA, aim at providing a picture of the potential impact at the level of the whole earthquake event. This scale is useful for rapidly sizing the disaster and for deciding at which level (e.g., regional, national, international) crisis management operations need to be activated, as well as the amount of aid and resources to dedicate. However, much more detailed information is needed very quickly: usually first responders require a detailed account of the situation at a local level, in order to establish in which street or building block to operate and to rescue potential casualties. Therefore, systems that estimate damage and losses at a more detailed resolution (e.g., SeisDaRo, ELER, SEISAID) constitute the strict minimum to meet these operational needs, although providing reliable results at such a scale remains very challenging. Conversely, it is not planned for the ShakeMap® and PAGER services to head in this direction, since these tools are intended for disaster management, not emergency response. As a result, the coupling between a shake-map system and a rapid loss assessment tool (at least at city district level) seems like the best way to go: shake-maps are able to provide updated ground-motion estimates, which can in turn feed fragility models of various structural types.
- Most rapid loss assessment systems are based on predicting damage to common buildings (residential or office types). Conversely, only a few of them consider infrastructure components or critical facilities (ShakeCast, SUPREME), and none of the current systems consider yet

the effect of failed components on the global performance of the infrastructure, which has a great influence on the crisis management operations (e.g., inaccessible roads, power outage, disrupted water supply). This crucial aspect requires further research efforts, since preliminary proof-of-concept studies have shown its potential [103], although modelling and computational issues need to be improved. Currently, the California Department of Transportation is also testing component-based fragilities in ShakeCast in addition to global functions [75].

- Furthermore, when carried out, the estimation of human impacts (fatalities, injuries, homeless people, etc.) is based on empirical methods that are often very simple. These consist either in directly applying predefined loss rate to the resident population according to the seismic intensity (PAGER), or in propagating predicted damages to building to their occupants (SIGE, SEISAid, ISARD) thanks to empirical conversion matrix and hypothesis about occupancy rate of buildings. Due to the criticality of the estimation of these human losses on decision-making in a crisis management context, further research should be conducted to reduce the associated uncertainty. For instance, by developing methodologies to model population exposure no longer as “static data” as is the case today, but as “dynamic data” taking into account hourly (accounting for pendulum movements) and seasonal (accounting for tourist populations) changes.
- Finally, while most recent shake-map systems show a strong focus on uncertainty treatment, such uncertainties are not propagated to the damage and loss assessment steps (i.e., generation of probabilistic distributions of loss metrics, accounting for all sources of variability). Although feasible in theory, one may wonder whether such a probabilistic framework would be of any use to decision makers, unless it could be easily communicated. Possible solutions could, for instance, follow rendering formats that are similar to the Earthquake Impact Scale [1,2] used in PAGER, which is as an effort to simplify the challenge of providing very uncertain fatality estimates.

## 5. Conclusions

This work provides an up-to-date inventory of current operating RRE systems with a particular focus on European ones, that includes details on their specific input and output data when the latter information is available. The tools used to assess damages and losses are also reviewed, and we discuss the shake-map algorithms implemented in the USGS ShakeMap® system and with the Bayesian Network approach.

A few weaknesses are identified, that concern the shake-map computation and the building inventories for loss and damage assessment. Amongst them, we mention the difficulty to take into account earthquakes specific characteristics (e.g. focal mechanism or directivity effect) into near-real time shake-map calculations. We stress the need to propagate carefully uncertainties from approximate site amplification factors or from GMMs and their epistemic selection. Furthermore, we remark that although the use of ‘social sensors’ (e.g. macroseismic testimonies on Twitter®) provides useful information for shake-map adjustment, more work is needed in order to use it efficiently in current algorithms. Nevertheless, the USGS ShakeMap® v4 system and the Bayesian Network approach are flexible enough to allow for such data to be implemented. They also prove more reliable than the USGS ShakeMap® v3.5 as they converge towards the same results, with a similar treatment of uncertainties. Concerning the loss assessment part, although most systems use mainly common building types for the inventories, the significantly bigger impact of some critical facilities (e.g. power plants or gas installations) and the likelihood of secondary risks associated needs to be reflected in the loss scenarios.

Another important point of the study is that while harmonization of RRE systems is desirable for using a robust shake-map algorithm taking into account the various data available with associated uncertainties, it is important to bear in mind that some inputs such as specific GMMs, soil

amplification factors and building inventories have to be provided at a local scale, in order for the resulting information to be useable by authorities. Moreover, the level of confidence that risk and disaster managers can have in such tools should be improved if these systems are also used in a planning and mitigation capacity (e.g., generation of prospective hazard and risk scenarios). For instance, USGS services (e.g., ShakeMap, ShakeCast, and PAGER) are not only tools for disaster operational management, but they are as important when used for exercises and planning via scenarios, as well as for risk studies and mitigation efforts. Most of the other damage and loss assessment tools presented in Table 4 have first been developed for planning and mitigation purposes, before being adapted to operate in a near real-time context.

Another important element that emerges from this study is the co-existence of RREs having international or even global coverage (e.g. USGS services) with others being rather country or regional specific, each with its own advantages. Thus, while the former are often technologically more robust (in terms of IT infrastructure, interoperability, service continuity, etc.) and can be validated very frequently in real situation, the latter allow, on the contrary, to take into account more detailed local specificities conditioning the estimation of losses (zoning of site effects, characterization of the vulnerability of buildings, etc.) as well as the particular needs of local stakeholders, but most often with a lack of validation and a operationality rather as demonstrators than as services. Finally, it is important to be aware that, as valuable as rapid response can be for crisis management, if it is not immediately understandable or if no operational implication follows naturally, it will be quickly dismissed and forgotten. Even beyond the cautious choice of indicators to provide, it is therefore also a question for the scientific community of making suitable choices in terms of information representation mode, semantics used, dissemination format, sequencing sending and versioning, etc. To overcome the well-known pitfall of “non-applicable applied research”, and with a view to favoring the operational declination of RREs (e.g. SIGE, ISARD, ...), it appears to be very important to involve stakeholders early in the development of these tools.

#### Author contributions

Simon Guérin-Marthe and Pierre Gehl wrote the core of the literature review. Simon Guérin-Marthe focused on the loss and damage assessment systems while Pierre Gehl worked more on the shake-map part. Samuel Auclair and Caterina Negulescu added informations concerning the state-of-the-art, in Part 3. Rosemary Fayjaloun reviewed the manuscript and edited parts of the text like in the introduction. All the authors read carefully the manuscript, made edits in the text and approved the final version.

#### Funding

This research was funded by the European Union's Horizon 2020 research and innovation program, grant number 821046.

#### Declaration of competing interest

The authors declare that they have no known competing financial interests or personal relationships that could have appeared to influence the work reported in this paper.

#### Acknowledgments

The authors thank Dr. David Wald and two other anonymous reviewers for their constructive comments which helped improving the accuracy and the quality of the manuscript. The authors are also very grateful to some colleagues of the TURNkey project who have provided much needed knowledge and insight on the systems operating in their

respective countries; namely Dr. Barbara Borzi and Dr. Francesca Bozzoni from EUCENTRE, Dr. Remy Bossu and Dr. Sylvain Julien-Laferrrière from EMSC, Dr. Florin Balan from INFP, and Dr. Jordi Domingo Ballesta from KNMI.

#### References

- [1] D.J. Wald, K.S. Jaiswal, K.D. Marano, D. Bausch, Earthquake impact scale, *Nat. Hazards Rev.* 12 (3) (2011), [https://doi.org/10.1061/\(ASCE\)NH.1527-6996.0000040](https://doi.org/10.1061/(ASCE)NH.1527-6996.0000040).
- [2] David J. Wald, V. Quitoriano, B. Worden, M. Hopper, J.W. Dewey, USGS “Did You Feel It?” internet-based macroseismic intensity maps, *Ann. Geophys.* 54 (6) (2011), <https://doi.org/10.4401/ag-5354>.
- [3] R. Fayjaloun, P. Gehl, F. Boulahya, S. Guerin-Marthe, A. Roullé, *International Journal of Disaster Risk Reduction* (2020).
- [4] P. Cronin, F. Ryan, M. Coughlan, Undertaking a literature review: a step-by-step approach, in: *British Journal of Nursing*, Mark Allen Publishing, 2008, <https://doi.org/10.12968/bjon.2008.17.1.28059>.
- [5] D. Wald, C.B. Worden, V. Quitoriano, K.L. Pankow, *ShakeMap® Manual*, Technical Manual, Users Guide, and Software Guide, 2006.
- [6] C.B. Worden, E.M. Thompson, J.W. Baker, B.A. Bradley, N. Luco, D. Wald, Spatial and spectral interpolation of ground-motion intensity measure observations, *Bull. Seismol. Soc. Am.* 108 (2) (2018) 866–875.
- [7] P. Gehl, J. Douglas, D. D’Ayala, Inferring earthquake ground-motion fields with Bayesian Networks, *Bull. Seismol. Soc. Am.* 107 (6) (2017).
- [8] M. Erdik, K. Sesetyan, M.B. Demircioglu, U. Hancilar, C. Zülfiqar, Rapid earthquake loss assessment after damaging earthquakes, *Soil Dynam. Earthq. Eng.* 31 (2) (2011) 247–266.
- [9] D. Wald, V. Quitoriano, T.H. Heaton, H. Kanamori, C.W. Scrivner, C.B. Worden, TriNet “ShakeMaps”: rapid generation of peak ground-motion and intensity maps for earthquakes in Southern California, *Earthq. Spectra* 15 (3) (1999) 537–556.
- [10] C.B. Worden, D. Wald, T. Allen, K.W. Lin, D. Garcia, G. Cua, A revised ground-motion and intensity interpolation scheme for ShakeMap, *Bull. Seismol. Soc. Am.* 100 (6) (2010) 3083–3096.
- [11] P.J. Stafford, Evaluation of structural performance in the immediate aftermath of an earthquake: a case study of the 2011 Christchurch earthquake, *Int. J. Forensic Eng.* 1 (1) (2012) 58–77.
- [12] E. Vanmarcke, *Random Fields, Analysis and Synthesis*, The MIT Press, 1983.
- [13] N. Jayaram, J.W. Baker, Correlation model for spatially distributed ground-motion intensities, *Earthq. Eng. Struct. Dynam.* 38 (15) (2009) 1687–1708.
- [14] J. Douglas, Inferred ground motions on Guadeloupe during the 2004 Les Saintes earthquake, *Bull. Earthq. Eng.* 5 (3) (2007) 363–376.
- [15] S.A. King, A. Hortacsu, G.C. Hart, Post-earthquake estimation of site-specific strong ground motion, in: *13th World Conference on Earthquake Engineering*, 2004.
- [16] A. Costanzo, Shaking maps based on cumulative absolute velocity and arias intensity: the cases of the two strongest earthquakes of the 2016–2017 central Italy seismic sequence, *ISPRS Int. J. Geo-Inf.* 7 (7) (2018), <https://doi.org/10.3390/ijgi7070244>.
- [17] D. Wald, T. Allen, Topographic slope as a proxy for seismic site conditions and amplification, *Bull. Seismol. Soc. Am.* 97 (5) (2007) 1379–1395.
- [18] A. Lemoine, J. Douglas, F. Cotton, Testing the applicability of correlations between topographic slope and  $V_s/30$  for Europe, *Bull. Seismol. Soc. Am.* 102 (6) (2012) 2585–2599.
- [19] D.C. Heath, D.J. Wald, C.B. Worden, E.M. Thompson, G.M. Smoczyk, A global hybrid VS30 map with a topographic slope-based default and regional map insets, *Earthq. Spectra* (2020), <https://doi.org/10.1177/8755293020911137>.
- [20] Y.M. Wu, W.T. Liang, H. Mittal, W.A. Chao, C.H. Lin, B.S. Huang, C.M. Lin, Performance of a low-cost earthquake early warning system (P-alert) during the 2016 ML 6.4 Meinong (Taiwan) earthquake, *Seismol. Res. Lett.* 87 (5) (2016) 1050–1059.
- [21] S. Pramono, T. Allen, C. Bugden, R. Pandhu, I. Nindya, H. Ghasemi, Towards real-time earthquake impact alerting in Indonesia, *Geol. Soc. Lond. Spec. Publ.* 441 (1) (2017) 167–178.
- [22] A. Schaefer, J. Daniell, F. Wenzel, Rapid Earthquake Impact Modelling—GPU-powered intensity modelling cartography in social media, in: *EGU General Assembly Conference*, 2018.
- [23] T. Allen, A. Carapetis, J. Bathgate, H. Ghasemi, T. Pejić, A. Moseley, Real-time community internet intensity maps and ShakeMaps for Australian earthquakes, Australian, in: *Earthquake Engineering Society 2019 Conference*, Nov 29 – Dec 1, Newcastle, NSW, 2019.
- [24] E. Al Khatibi, K.M. Abou Elenean, A.S. Megahed, I. El-Hussain, Improved characterization of local seismicity using the Dubai Seismic Network, United Arab Emirates, *J. Asian Earth Sci.* 90 (2014), <https://doi.org/10.1016/j.jseas.2014.04.009>.
- [25] C. Cauzzi, J. Clinton, L. Faenza, S. Heimers, M. Koymans, V. Lauciani, R. Sleeman, ShakeMapEU: towards an integrated European ShakeMap system, in: *EGU General Assembly Conference*, 2018.
- [26] C. Cauzzi, B. Edwards, D. Fäh, J. Clinton, S. Wiemer, P. Kästli, D. Giardini, New predictive equations and site amplification estimates for the next-generation Swiss ShakeMaps, *Geophys. J. Int.* 200 (1) (2014) 421–438.
- [27] C. Marreiros, F. Carrilho, The ShakeMap at the Instituto de Meteorologia, in: *15th World Conference on Earthquake Engineering*, 2012.

- [28] C. Zulfikar, N.O.Z. Fercan, S. Tunc, M. Erdik, Real-time earthquake shake, damage, and loss mapping for Istanbul metropolitan area, *Earth Planets Space* 69 (1) (2017).
- [29] D. Toma-Danila, C.O. Ciaflan, C. Ionescu, A. Tigănescu, The near real-time system for estimating the seismic damage in Romania (SeisDaRo). Recent upgrades and results, in: 16th European Conference on Earthquake Engineering, 2018.
- [30] D. Bertil, J. Roviro, J.A. Jara, T. Susagna, E. Nus, X. Goula, B. Colas, G. Dumont, L. Cabanas, R. Anton, M. Calvet, ShakeMap implementation for Pyrénées in France-Spain border: regional adaptation and earthquake rapid response process, in: 15th World Conference on Earthquake Engineering, 2012.
- [31] Antoine Schlupp, ShakeMap fed by macroseismic data in France: feedbacks and contribution for improving SHA, in: AGU Fall Meeting 2016, 2016.
- [32] A. Schlupp, M. Grunberg, D. Bertil, M. Schaming, A. Ulrich, Les « ShakeMap » pour les territoires français : un produit pour la gestion de crise et un outil R&D pour l'estimation de l'aléa, in: 10ème Colloque National AFPS, 24-27 Septembre 2019, Strasbourg, 2019.
- [33] F. Bosco, A. Deschamps, S. Auclair, Rapid Assessment of Seismic Impact in Western Alpine Area: Development in Italy and French Cross-Border Project (ALCOTRA RISVAL). 38<sup>e</sup> Convegno Nazionale GNGTS (Roma, 12-14 Novembre 2019), 2019.
- [34] A. Michelini, L. Faenza, V. Lauciani, L. Malagnini, ShakeMap implementation in Italy, *Seismol Res. Lett.* 79 (5) (2008) 689–698.
- [35] K.T. Shabestari, F. Yamazaki, A proposal of instrumental seismic intensity scale compatible with MMI evaluated from three-component acceleration records, *Earthq. Spectra* 17 (4) (2001) 711–723.
- [36] V. De Rubeis, P. Sbarra, P. Tosi, D. Sorrentino, Hai Sentito Il Terremoto (HSIT)—macroseismic Intensity Database 2007–2018, 2019 version 1.
- [37] B. Colas, A. Roullé, M. Terrier, Macrozonage sismique des Pyrénées-Orientales. Rapport final, BRGM/RP-62994-FR, 2013.
- [38] J. Régnier, E. Bertrand, H. Cadet, Repeatable process for seismic microzonation using 1-D site-specific response spectra assessment approaches. Application to the city of Nice, France, *Eng. Geol.* 270 (2020), <https://doi.org/10.1016/j.enggeo.2020.105569>.
- [39] R.D. Borcherdt, Estimates of site-dependent response spectra for design (methodology and justification), *Earthq. Spectra* 10 (4) (1994), <https://doi.org/10.1193/1.1585791>.
- [40] G.M. Calvi, R. Pinho, G. Magenes, J.J. Bommer, L.F. Restrepo-Vélez, H. Crowley, Development of seismic vulnerability assessment methodologies over the past 30 years, *ISET J. Earthq. Technol.* (2006).
- [41] R.V. Whitman, T. Anagnos, C.A. Kircher, H.J. Lagorio, R.S. Lawson, P. Schneider, Development of a national earthquake loss estimation methodology, *Earthq. Spectra* (1997), <https://doi.org/10.1193/1.1585973>.
- [42] D. Benedetti, V. Petrini, Sulla vulnerabilità sismica di edifici in muratura: proposta su un metodo di valutazione, *L'Industria Delle Costruzioni* (1984).
- [43] S.V. Medvedev, W. Sponheuer, Scale of seismic intensity, in: Proc. IV World Conference of the Earthquake Engineering, 1969.
- [44] A.J. Kappos, K. Pitilakis, K.C. Stylianidis, Cost-benefit analysis for the seismic rehabilitation of buildings in Thessaloniki, based on a hybrid method of vulnerability assessment, in: Fifth International Conference on Seismic Zonation (Nice), 1995, pp. 406–413.
- [45] A.H. Barbat, F.Y. Moya, J.A. Canas, Damage Scenarios Simulation for Seismic Risk Assessment in Urban Zones. *Earthquake Spectra*, 1996, <https://doi.org/10.1193/1.1585889>.
- [46] A. Bernardini, La Vulnerabilità Degli Edifici: Vatuazione a Scala Nazionale Della Vulnerabilità Sismica Degli Edifici Ordinari. *Research Report*, CNR-Gruppo Nazionale per La Difesa Dai Terremoti, Rome, Italy, 2000 (in Italian).
- [47] D. D'Ayala, E. Speranza, An Integrated Procedure for the Assessment of Seismic Vulnerability of Historic Buildings. *12th European Conference on Earthquake Engineering*, 2002.
- [48] S.A. Freeman, The capacity spectrum method as a tool for seismic design, in: 11th European Conference on Earthquake Engineering, 1998.
- [49] Gian Michele Calvi, A displacement-based approach for vulnerability evaluation of classes of buildings, *J. Earthq. Eng.* (1999), <https://doi.org/10.1080/13632469909350353>.
- [50] N. Makhoul, S. Argyroudis, Loss estimation software: developments, limitations and future needs, in: 16th European Conference on Earthquake Engineering, 2018.
- [51] U. Hancilar, C. Tuzun, C. Yenidogan, M. Erdik, O. Katz, ELER software—a new tool for urban earthquake loss assessment, *Nat. Hazards Earth Syst. Sci.* 10 (12) (2010).
- [52] S. Molina, D.H. Lang, C.D. Lindholm, SELENA—An open-source tool for seismic risk and loss assessment using a logic tree computation procedure, *Comput. Geosci.* 36 (3) (2010) 257–269.
- [53] H. Crowley, R. Pinho, J.J. Bommer, J.F. Bird, Development of a Displacement-Based Method for Earthquake Loss Assessment, 2006.
- [54] B. Borzi, H. Crowley, R. Pinho, Simplified pushover-based earthquake loss assessment (SP-BELA) method for masonry buildings, *Int. J. Architect. Herit.* 2 (4) (2008) 353–376.
- [55] O. Sedan, C. Negulescu, M. Terrier, A. Roullé, T. Winter, D. Bertil, Armagedom—a tool for seismic risk assessment illustrated with applications, *J. Earthq. Eng.* 17 (2) (2013) 253–281.
- [56] Z. Milutinovic, G. Trendafiloski, Risk-UE an Advanced Approach to Earthquake Risk Scenarios with Applications to Different European Towns. Report to WP4: Vulnerability of Current Buildings, 2003.
- [57] G. Grunthal, European Macroseismic Scale EMS - 98, vol. 15, Conseil de l'Europe, 1998.
- [58] S. Giovinazzi, S. Lagomarsino, A macroseismic method for the vulnerability assessment of buildings, in: 13th World Conference on Earthquake Engineering, 2004.
- [59] FEMA, HAZUS-MH Technical Manual, 2003.
- [60] P. Lestuzzi, S. Podestà, C. Luchini, A. Garofano, D. Kazantzidou-Firtinidou, C. Bozzano, P. Bischof, A. Haffter, J.D. Rouiller, Seismic vulnerability assessment at urban scale for two typical Swiss cities using Risk-UE methodology, *Nat. Hazards* (2016), <https://doi.org/10.1007/s11069-016-2420-z>.
- [61] V. Silva, H. Crowley, M. Pagani, D. Monelli, R. Pinho, Development and application of OpenQuake, an open source software for seismic risk assessment, in: 15th World Conference on Earthquake Engineering, Lisbon, Portugal, 2012.
- [62] B. Tang, Q. Chen, X. Liu, Z. Liu, Y. Liu, J. Dong, L. Zhang, Rapid estimation of earthquake fatalities in China using an empirical regression method, *Int. J. Disaster Risk Reduct.* 41 (2019), <https://doi.org/10.1016/j.ijdr.2019.101306>.
- [63] S.T. Maqsood, J. Schwarz, Estimation of human casualties from earthquakes in Pakistan - an engineering approach, *Seismol Res. Lett.* 82 (1) (2011), <https://doi.org/10.1785/gssrl.82.1.32>.
- [64] K.S. Jaiswal, D.J. Wald, P.S. Earle, K.A. Porter, M. Hearne, Earthquake casualty models within the USGS prompt assessment of global earthquakes for response (PAGER) system, in: Advances in Natural and Technological Hazards Research, vol. 29, 2011, [https://doi.org/10.1007/978-90-481-9455-1\\_6](https://doi.org/10.1007/978-90-481-9455-1_6).
- [65] Kishor S. Jaiswal, D.J. Wald, Development of a semi-empirical loss model within the USGS prompt assessment of global earthquakes for response (PAGER) system, in: 9th US National and 10th Canadian Conference on Earthquake Engineering 2010, 2010.
- [66] J. Cousins, G.N.S. Science, L. Hutt, N. Zealand, Estimated Casualties in New Zealand Earthquakes, *Statistics*, 1998.
- [67] K.A. Porter, K.S. Jaiswal, D.J. Wald, P.S. Earle, M. Hearne, Patality models for the U.S. Geological survey's prompt assessment of global earthquakes for response (PAGER) system, in: The 14 Th World Conference on Earthquake Engineering, 2008.
- [68] A. Coburn, R. Spence, Earthquake Protection, John Wiley, 1992, <https://doi.org/10.5459/bnzsee.27.2.163>.
- [69] R. Spence, LESSLOSS Report 2007/07: Earthquake Disaster Scenario Predictions and Loss Modelling for Urban Areas, 2007.
- [70] H. Jia, J. Lin, J. Liu, An earthquake fatalities assessment method based on feature importance with deep learning and random forest models, *Sustainability* 11 (10) (2019), <https://doi.org/10.3390/su11102727>.
- [71] R. Hingorani, P. Tanner, M. Prieto, C. Lara, Consequence classes and associated models for predicting loss of life in collapse of building structures, *Struct. Saf.* 85 (2020), <https://doi.org/10.1016/j.strusafe.2019.101910>.
- [72] M. gobatto, W.M. Yeo, N. Shome, Uncertainty quantification and sensitivity analysis of earthquake casualties, in: NCEE 2014 - 10th U.S. National Conference on Earthquake Engineering: Frontiers of Earthquake Engineering, 2014, <https://doi.org/10.4231/D3639K592>.
- [73] D. Wald, K. Jaiswal, K.D. Marano, D.B. Bausch, M.G. Hearne, PAGER — Rapid Assessment of an Earthquake's Impact, 2010.
- [74] K. Jaiswal, D. Wald, K. Porter, A Global Building Inventory for Earthquake Loss Estimation and Risk Management, *Earthquake Spectra*, 2010.
- [75] K. Lin, D.J. Wald, C.A. Kircher, D. Slosky, K. Jaiswal, N. Luco, USGS shakecast system advancements, in: 11th National Conference on Earthquake Engineering 2018, NCEE 2018: Integrating Science, Engineering, and Policy, vol. 6, 2018, pp. 3458–3468.
- [76] S. Auclair, D. Monfort, B. Colas, T. Langer, D. Bertil, Outils de réponse rapide pour la gestion opérationnelle de crises sismiques, Colloque SAGEO (2014).
- [77] S. Auclair, D. Monfort, B. Colas, T. Langer, P. Perrier, Evaluation rapide des bilans matériels et humains: une aide essentielle à la gestion opérationnelle des crises sismiques, 9ème Colloque National AFPS (2015).
- [78] S. Auclair, F. Boulahya, B. Birregah, R. Quique, R. Ouaret, E. Soulier, SURICATE-Nat: innovative citizen centered platform for Twitter based natural disaster monitoring, in: 6th International Conference on Information and Communication Technologies for Disaster Management, 2019, <https://doi.org/10.1109/ICT-DM47966.2019.9032950>, ICT-DM 2019.
- [79] G. Trendafiloski, M. Wyss, P. Rosset, Loss estimation module in the second generation software QLARM, in: Human Casualties in Earthquakes, Springer, Dordrecht, 2011, pp. 95–106.
- [80] G. Di Pasquale, G. Orsini, R.W. Romeo, New developments in seismic risk assessment in Italy, *Bull. Earthq. Eng.* 3 (1) (2005) 101–128.
- [81] M. Faravelli, B. Borzi, M. Pagano, D. Quaroni, Using OpenQuake to define seismic risk and real time damage scenario in Italy, in: 16th European Conference on Earthquake Engineering, 2018.
- [82] B. Borzi, A. Di Meo, M. Faravelli, E. Fiorini, M. Onida, Mappe di rischio sismico e scenario per gli edifici scolastici italiani. *XIV Convegno L'Ingegneria Sismica in Italia ANDIS*, 2011.
- [83] B. Borzi, A. Di Meo, M. Faravelli, E. Fiorini, M. Onida, Definizione di una procedura di prioritizzazione per interventi di mitigazione del rischio degli edifici scolastici. *XIV Convegno L'Ingegneria Sismica in Italia ANDIS*, 2011.
- [84] F. Bozzoni, C.G. Lai, P. Marsan, D. Conca, A. Fama, WebGIS platform for seismic risk assessment of maritime port systems in Italy, in: 4th PIANC Mediterranean Days Congress, 2018.
- [85] A. Di Meo, B. Borzi, D. Quaroni, M. Onida, V. Pascale, Real-time damage scenario and seismic risk assessment of Italian roadway network, in: 16th European Conference on Earthquake Engineering, 2018.
- [86] F. Bozzoni, C.G. Lai, A. Balia, A.G. Ozebe, D. Khairy, Stochastic ground response analyses at an international airport in northern Italy, in: 23rd International Conference on Computer Methods in Mechanics, 2019.

- [87] S. Gilles, Utilization of ELER V2 and Improvement of ESMC Earthquake Impact Estimation Method, 2010.
- [88] S. Julien-Laferrrière, Earthquake Qualitative Impact Assessment – Performance Evaluation, 2019.
- [89] C.H. Yeh, C.H. Loh, K.C. Tsai, Overview of Taiwan earthquake loss estimation system, *Nat. Hazards* 37 (1–2) (2006) 23–37.
- [90] S. Midorikawa, Dense strong-motion array in Yokohama, Japan, and its use for disaster management, in: *Directions in Strong Motion Instrumentation*, Springer, Dordrecht, 2005, pp. 197–208.
- [91] Y. Shimizu, F. Yamazaki, R. Isoyama, E. Ishida, K. Koganemaru, W. Nakayama, Development of realtime disaster mitigation system for urban gas supply network, in: *13th World Conference on Earthquake Engineering*, 2004.
- [92] X. Goula, P. Dominique, B. Colas, J.A. Jara, A. Roca, T. Winter, Seismic rapid response system in the Eastern Pyrenees, in: *XIV World Conference on Earthquake Engineering*, 12–17, 2008.
- [93] D.L. Wells, K.J. Coppersmith, New empirical relationships among magnitude, rupture length, rupture width, rupture area, and surface displacement, *Bull. - Seismol. Soc. Am.* (1994).
- [94] E.M. Thompson, C.B. Worden, Estimating rupture distances without a rupture, *Bull. Seismol. Soc. Am.* 108 (1) (2018), <https://doi.org/10.1785/0120170174>.
- [95] B. Rowshandel, Directivity correction for the next generation attenuation (NGA) relations, *Earthq. Spectra* (2010), <https://doi.org/10.1193/1.3381043>.
- [96] V. Convertito, M. Caccavale, R. de Matteis, A. Emolo, D. Wald, A. Zollo, Fault Extent Estimation for Near-Real-Time Ground-Shaking Map Computation Purposes, *Bulletin of the Seismological Society of America*, 2012, <https://doi.org/10.1785/0120100306>.
- [97] M. Pagani, D. Monelli, G. Weatherill, L. Danciu, H. Crowley, V. Silva, P. Henshaw, L. Butler, M. Nastasi, L. Panzeri, M. Simionato, D. Viganò, Openquake engine: an open hazard (and risk) software for the global earthquake model, *Seismol Res. Lett.* 85 (3) (2014) 692–702, <https://doi.org/10.1785/0220130087>.
- [98] D. García, D.J. Wald, M.G. Hearne, A Global Earthquake Discrimination Scheme to Optimize Ground-Motion Prediction Equation Selection, *Bulletin of the Seismological Society of America*, 2012, <https://doi.org/10.1785/0120110124>.
- [99] C.B. Worden, D. Wald, *ShakeMap Manual Online: Technical Manual, User's Guide, and Software Guide*, 2020.
- [100] Vitor Silva, N. Horspool, Combining USGS ShakeMaps and the OpenQuake-engine for damage and loss assessment, *Earthq. Eng. Struct. Dynam.* 48 (6) (2019) 634–652, <https://doi.org/10.1002/eqe.3154>.
- [101] R. Bossu, F. Roussel, L. Fallou, M. Landès, R. Steed, G. Mazet-Roux, A. Dupont, L. Probert, L. Petersen, LastQuake: from rapid information to global seismic risk reduction, *Int. J. Disaster Risk Reduct.* (2018), <https://doi.org/10.1016/j.ijdr.2018.02.024>.
- [102] F. Finazzi, The Earthquake Network Project: toward a Crowdsourced Smartphone-Based Earthquake Early Warning System, *Bulletin of the Seismological Society of America*, 2016, <https://doi.org/10.1785/0120150354>.
- [103] P. Gehl, F. Cavalieri, P. Franchin, Approximate Bayesian network formulation for the rapid loss assessment of real-world infrastructure systems, *Reliab. Eng. Syst. Saf.* 177 (April) (2018) 80–93, <https://doi.org/10.1016/j.res.2018.04.022>.



## **Update**

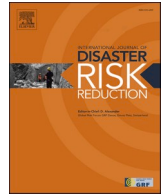
# **International Journal of Disaster Risk Reduction**

Volume 57, Issue , 15 April 2021, Page

DOI: <https://doi.org/10.1016/j.ijdrr.2021.102256>

Contents lists available at [ScienceDirect](https://www.sciencedirect.com)

## International Journal of Disaster Risk Reduction

journal homepage: <http://www.elsevier.com/locate/ijdr>

## Corrigendum to “Rapid earthquake response: The state-of-the art and recommendations with a focus on European systems” [Int. J. Disaster Risk Reduct. 52 (2020) 101958]

Simon Guérin-Marthe<sup>\*</sup>, Pierre Gehl, Caterina Negulescu, Samuel Auclair, Rosemary Fayjaloun

BRGM, Orléans Cedex, France

The authors would like to report some inaccuracies found in their paper. The following points should be corrected:

1. The ELER methodology and software described in section 3.2.1.5 of the paper is operational both at the country scale, and at the city scale (for Istanbul only). The operations differ for these two cases:

- At the country scale, immediately after an earthquake in and around Turkey, intensity shakemaps are automatically generated by ELER and published by KOERI-RETMC (<http://www.koeri.boun.edu.tr/sismo/2/latest-earthquakes/rapid-intensity-maps/>). Then, as recorded ground-motion data become available, bias adjusted shakemaps and intensity based building damage estimation maps are manually reproduced (e.g. <https://twitter.com/BUDEpremMuh/status/1323369845>

[220610049](https://doi.org/10.1016/j.ijdr.2020.101958)).

- In the case of Istanbul, it is a separate system that does not use the KOERI-RETMC shakemaps. Instead, ELER produces PGA, PGV, Sa and intensity shakemaps, incorporating recorded strong ground-motion data by IEEWRRS (<https://eqe.boun.edu.tr/en/istanbul-earthquake-rapid-response-and-early-warning-laboratory>). The Vs30 based on local soil information is also taken into account. Then, spectral acceleration-displacement based building damage estimation maps are produced (e.g. <https://eqe.boun.edu.tr/en/26-september-2019-1359-istanbul-silivri-earthquake>).

2. In Reference [51], O. Katz is not an author of the paper.

The authors would like to apologise for any inconvenience caused.

DOI of original article: <https://doi.org/10.1016/j.ijdr.2020.101958>.

<sup>\*</sup> Corresponding author.

E-mail address: [simon-gm@hotmail.fr](mailto:simon-gm@hotmail.fr) (S. Guérin-Marthe).

<https://doi.org/10.1016/j.ijdr.2021.102256>

Available online 12 April 2021

2212-4209/© 2020 The Author(s). Published by Elsevier Ltd. This is an open access article under the CC BY license (<http://creativecommons.org/licenses/by/4.0/>).